

ELECTRODE KINETIC STUDIES USING A COMPUTERIZED  
DATA ACQUISITION AND ANALYSIS SYSTEM

Thesis by

Roger Henry Abel

In Partial Fulfillment of the Requirements

For the Degree of

Doctor of Philosophy

California Institute of Technology

Pasadena, California

1971

(Submitted November 30, 1970)

## Acknowledgments

I am indebted to my research adviser, Dr. Fred Anson, for helping to make my graduate study a rewarding and stimulating experience. I wish to acknowledge the invaluable assistance and suggestions that he has given me and the untiring patience he has shown toward me. I wish to also acknowledge the aid and friendship I have received from Dr. George Lauer, Dr. Donald Barclay, Hong Sup Lim and the other members of Dr. Anson's research group.

I wish also to acknowledge the financial aid that has been provided for me by the Institute and by the Danforth Foundation and National Science Foundation in the form of predoctoral fellowships.

Finally, I would like to dedicate this thesis to my wife and my parents as an acknowledgment of their contributions.

## Abstract

The first section of this dissertation introduces the basic concepts that are necessary for the quantitative description of electrode kinetics. The refinements and corrections in the rate equation that are due to a detailed model of the electrical double layer, and to the potential step relaxation technique are introduced and discussed.

A discussion of the non-linear statistical analysis techniques that are necessary for a rigorous analysis of rate equation is presented in the second section. The estimates of the precision of the desired parameters obtained by using statistical methods can be used as a measure of the efficiency of an experiment. Their use as measures of "kinetic information density" is developed and illustrated by comparing charge and current measurement in the potential step technique. Previous approaches to the subject of "kinetic information density" are discussed and compared to the results from statistical analysis.

The third section describes the computerized data acquisition and analysis system that was designed and used for the study of electrode kinetics.

The final section presents the results of the kinetic studies undertaken on the  $Zn^{+2}/Zn(Hg)$  system in 1 F  $NaNO_3$ , 1 F  $NaClO_4$ , and 1 F  $NaCl$  supporting electrolytes. Ensemble averaging is used in these studies to increase precision and its values is illustrated.

The results that are obtained for the rate constants in the various supporting electrolytes are compared and it is shown that the rates are comparable in  $\text{NaNO}_3$  and  $\text{NaClO}_4$  supporting electrolytes but significantly greater in 1 F  $\text{NaCl}$ . These results are compared with results of previous investigators and the quality of the results of this thesis are compared to those of previous investigators.

## TABLE OF CONTENTS

	<u>Page</u>
Acknowledgments	ii
Abstract	iii
I. Electrode Kinetics: Introduction and Development of the Rate Equation	1
Introduction to Electrode Kinetics	2
Basic Theory of Electrode Kinetics	7
The Double Layer and Electrode Kinetics	12
The Potential Step Method, Mass Transfer Considerations	18
II. Utilization of Statistical Techniques in Electrode Kinetics Experiments	21
Statistical Analysis of Kinetic Data	22
Statistics and Kinetic Information Density	28
III. Acquisition and Analysis of Kinetic Data by a Digital Computer	50
IV. Investigation of the $Zn^{+2}/Zn(Hg)$ Electrode Reaction in 1 <u>F</u> $NaNO_3$ , 1 <u>F</u> $NaClO_4$ , and 1 <u>F</u> $NaCl$	62
Experimental Conditions	63
Experimental Results	69
Discussion	93

	<u>Page</u>
References	100
Appendix A	104
Appendix B	108
Propositions	116

## TABLE OF FIGURES

<u>Figure</u>		<u>Page</u>
1	A pictorial representation of the electrical double layer	14
2	Kinetic information as a function of time and potential for the measurement of current and charge using the potential step method	37
3	Potential dependence of the variance-covariance matrix elements relating to the parameter, Kappa	43
4	Potential dependence of the variance-covariance matrix elements relating to the parameter, Lambda	45
5	Relative expected imprecision of Kappa for charge and current measurement as a function of potential	47
6	A block diagram of the computerized data acquisition and analysis system	53
7	Time sequence diagram depicting signals and events occurring in a typical kinetic experiment	60
8	Experimental results for $Q_{dl}$ obtained from kinetic experiments	77
9	Experimental results for Lambda obtained from kinetic experiments	79
10	Experimental results for Kappa obtained from kinetic experiments	81

**I. Electrode Kinetics: Introduction and Development of  
the Rate Equation**

## Introduction to Electrode Kinetics

Charge transfer reactions occurring between an electrode and a chemical species in solution are heterogeneous reactions. The rates of these reactions are profoundly affected by the conditions in the region of the solution-electrode interface. This type of reaction has been of interest for some time and several books and articles are available which deal with both theoretical and practical aspects of this subject (1-9).

When relaxation methods are used to study the kinetics of charge transfer reactions, not only must one take into account the state of the interfacial region but also the rate and means of transport of the reacting species to the reaction site (the electrode) must be considered. By choosing appropriate experimental conditions, e.g., a large excess of indifferent ions and relatively short experimental times, transfer of the reacting species to the electrode by migration and convection can be neglected. Transfer of the reacting species then takes place solely by diffusion, usually linear and semi-infinite. As long as the rate of the charge transfer reaction is controlled primarily by the kinetics of the charge transfer, information can be obtained about these kinetics, but when the rate of the charge transfer reaction becomes limited by the rate at which reacting species can diffuse from the solution to the electrode no information can be gained about the kinetics of the actual charge transfer occurring between the species of interest and the electrode. At the start of any experiment the concentration of the

reacting species is uniform throughout the solution. After the experiment is initiated, it is often possible to assume that the initial uniform concentration is maintained for short times. However, after the reaction has proceeded sufficiently, the reacting species will become depleted at the electrode and a concentration gradient will be set up which will cause reactant in the solution to diffuse to the electrode. Thus the rate of the reaction is controlled primarily by the rate of the charge transfer process at short times, while at longer times, diffusion becomes more and more important and eventually the rate of the reaction will be determined entirely by the rate of diffusion of the reacting species to the electrode. One can discuss three time ranges in an experiment. In the first, the rate of the reaction is controlled by the rate of charge transfer, in the second there is mixed control by diffusion and charge transfer, and in the third range the rate of the reaction is controlled by the rate of diffusion of the reacting species.

In the past, it has been commonplace to attempt to obtain all of the data in the first-time range so that the effects of diffusion can be neglected and a simplified model employed in analysis of the data. However, conditions where the simplified analysis can be made prove to be very restrictive in terms of the time range that is available and the magnitude of the charge transfer rates that can be measured. The time range over which diffusion may be neglected and the rate of the charge transfer reaction are coupled so that the faster the rate of the charge transfer reaction the smaller the time range that is available before diffusion becomes important. The fastest

reactions are partially controlled by diffusion even at the shortest times that are available to the experimenter and for these reactions the effect of diffusion on the overall rate must be taken into account to obtain valid estimates of the rate of charge transfer. The equations which are applicable to this situation are nonlinear in the parameters which are to be determined and thus linear least-squares analysis techniques of the types generally employed cannot be used. Previous workers have generally avoided the rigorous analysis and have used instead simplified, approximate models for the more complex rigorous equations. While this approach does make possible the study of rates of charge transfer that are faster than can be accommodated with the first approach, it still leads to quite restrictive experimental conditions. In addition, there is a real danger that the approximate equations will be applied under circumstances where they are not applicable (10). The use of simplified approximations was well justified when analysis of the data was undertaken using manual or desk computation, however because of the ready availability of computers today, the rigorous equations, even though they are nonlinear, do not present a major problem for analysis.

Using the rigorous equations to analyze the data obtained in an experiment makes it possible to get valid estimates of the rate of a charge transfer reaction even under conditions where the rate of the overall reaction is partially controlled by the rate of diffusion of the reacting species to the electrode. When the rate of the reaction becomes essentially completely controlled by the rate of diffusion,

no more information about the rate of the charge transfer process is obtainable. The point in time at which this change from partial control to full control by the rate of diffusion takes place is not well defined, rather it is a gradual change and is largely determined by the accuracy and precision with which one can obtain the data. That is, the more precise the data that are obtained, the higher the rate of charge transfer one can measure before one must consider the reaction to be diffusion controlled. Even a computerized data analysis will not yield improved results unless the data being analyzed are sufficiently accurate and precise.

In order to optimize the experimental situation, we set out to develop a computerized system which could control the experiment, obtain highly precise data, and analyze the data using a rigorous analysis. The previous discussion has illustrated some of the general reasons why it was thought that the development of a computerized data acquisition and analysis system would prove a valuable tool for studies of electrode kinetics. The need for improvements in accuracy made possible by the development of the computerized data system can be illustrated by reference to the electrode reaction that was chosen for study in this thesis. The rate of the reduction of zinc has been measured previously by many investigators (11-18). The agreement among the results, however, has been disappointing. Even for apparently identical experimental conditions, e. g., 1 M KCl for a supporting electrolyte, values of the apparent rate constant reported have varied from  $4 \times 10^{-3}$  to  $16 \times 10^{-3}$  cm/sec (12, 13). Because of

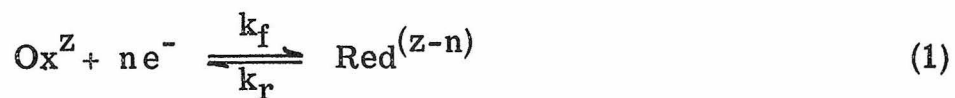
this divergence in the results and the resulting uncertainty in the absolute values of the rates, conclusions that are drawn concerning small variations in the rate constant that occur in different supporting electrolytes, or at different temperatures, etc. are not very convincing. Even though there is a lack of reproducibility of results that have been reported, several investigators have reported that the rate constant for the reduction of zinc varies with supporting electrolyte used (14-18). The rate of the reaction appears to become greater when chloride is substituted for nitrate or perchlorate and the enhancement of the rate when bromide is used appears to be even greater than with chloride. The reduction of zinc in various supporting electrolytes was chosen for study because this reaction displays a rate that is in a convenient range to study and there are ample previous data with which to compare our data. The potential range over which the zinc reduction may be studied is sufficiently negative that adsorption of perchlorate or nitrate anions, two of the supporting electrolytes employed, is small or negligible (15). Also, specific adsorption of zinc ion does not appear to occur in these electrolytes (15).

## Basic Theory of Electrode Kinetics

Before discussing the experiments and results in detail, some of the basic ideas of electrode kinetics will be presented and applied to the particular relaxation technique that was used in these investigations. The aim in presenting these basic ideas on electrode kinetics is not to be exhaustive but rather to provide those concepts which are necessary for latter discussions. For a more thorough development of these ideas the reader is referred to Delahay's, "Double Layer and Electrode Kinetics" (2).

In this presentation we will make several assumptions which will be mentioned before proceeding further. Because the activities of the species in solution are generally not available, their activities will be approximated by concentrations. If the activities do happen to be known the resulting equations in concentration terms can be simply corrected. Another assumption that we will make initially is that the reacting species can reach the electrode as fast as necessary to maintain a uniform concentration throughout the solution, i. e., the rate of diffusion will be assumed to be very fast compared to the rate of electron transfer. This assumption enables us to neglect the mass-transfer process and concentrate on a description of the charge transfer process itself. Later when discussing the relaxation technique that was used for the kinetic studies this assumption will be discarded and the mass-transfer aspects of the kinetics will be dealt with. However, utilization of this assumption enables us to discuss

and develop kinetic equations which are general and independent of the technique chosen to study the kinetics. The reaction to be described (Eq. (1)) is assumed to be first order in the reacting species and it is assumed that the number of electrons transferred in the overall reaction (n) are transferred during the rate-determining step.



where  $\text{Ox}^z$  is the oxidized species with a charge of  $z$ , Red is the reduced species which has a charge of  $(z-n)$ , and  $n$  is the number of electrons involved in the charge transfer reaction. Reaction (1) is a first-order heterogeneous reaction, the rate of which is expressed in units of moles/cm<sup>2</sup>/sec. The heterogeneous rate constants,  $k_f$  and  $k_r$ , have units of cm/sec.

$$\begin{aligned} \text{Rate} &= -\frac{d[\text{Ox}^z]}{dt} = \frac{d[\text{Red}^{(z-n)}]}{dt} \\ &= k_f[\text{Ox}^z] - k_r[\text{Red}^{(z-n)}] \quad (2) \end{aligned}$$

The rate is more conveniently expressed and measured in terms of current density,  $i$ , obtained by multiplication of the rate by the number of electrical equivalents per mole:

$$i = nF \text{ (Rate)} \quad (3)$$

where  $n$  is the number of equivalents per mole and  $F$  is the Faraday

constant. Reduction current is taken as positive and oxidation current negative (2). The rate constants,  $k_f$  and  $k_r$ , will differ from ordinary chemical rate constants because they will be strongly influenced by the electrical field that is present at the electrode-solution interface, i. e., they will depend on the electrode potential.

The theoretical equations that describe the rate process occurring at the electrode can be developed analogously to the non-electrochemical case with the exception that the standard free energy of activation becomes a standard electrochemical free energy of activation, which is dependent on the potential difference at the electrode solution interface. The standard electrochemical free energy of activation,  $\Delta\bar{G}^0\ddagger$ , is described by the following equation (19)

$$\Delta\bar{G}^0\ddagger = \Delta G_c^0\ddagger + \alpha n F E \quad (4)$$

where  $\Delta G_c^0\ddagger$  is the standard chemical free energy of activation and  $\alpha$  is a number having a value between zero and one. This fraction,  $\alpha$ , is called the symmetry factor (20), and the term  $\alpha n F E$  is the fraction of the electrical energy  $n F E$  where  $E$  is the potential difference between electrode and solution that contributes to the standard free energy of activation for the forward reaction (reduction). Similarly,  $(1 - \alpha)nFE$  measures this contribution in the reverse direction (oxidation).

The rate equation can then be written in a form where the rate is an explicit function of the potential and new rate constants,  $k_c$  and

$k_a$ , may be defined which are independent of the potential. The rate expression then becomes:

$$i = nF \left\{ [Ox] k_c \exp\left[-\frac{\alpha nFE}{RT}\right] - [Red] k_a \exp\left[\frac{(1-\alpha)nFE}{RT}\right] \right\} \quad (5)$$

where  $[Ox]$  and  $[Red]$  are the concentrations of the oxidized and reduced species at the reaction sites and  $E$  is the potential of the electrode versus some reference electrode. The rate constants defined in this way depend on the particular reference electrode used, and it is more meaningful to derive expressions for rate constants which are independent of the particular reference electrode used. To do this, we must consider the system under equilibrium conditions with both reactants in their standard states. Under these conditions, there is no net current and the potential at the electrode interface is the standard potential,  $E^0$ , for the particular redox couple under consideration.

Since there is no net current and since both  $O$  and  $Red$  are in their standard states Eq. (5) may be written:

$$i = 0 = nF \left( k_c \exp\left[-\frac{\alpha nFE^0}{RT}\right] - k_a \exp\left[\frac{(1-\alpha)nFE^0}{RT}\right] \right) \quad (6)$$

$$k_c \exp\left[-\frac{\alpha nFE^0}{RT}\right] = k_a \exp\left[\frac{(1-\alpha)nFE^0}{RT}\right] \equiv k_s^a \quad (6a)$$

By using the above definition for the apparent standard rate constant,  $k_s^a$ , the current density at any potential may be written as

follows:

$$i = nFk_s^a \left[ [Ox] \exp \left\{ -\frac{\alpha nF}{RT} (E - E^0) \right\} - [Red] \exp \left\{ \frac{(1-\alpha)nF}{RT} (E - E^0) \right\} \right] \quad (7)$$

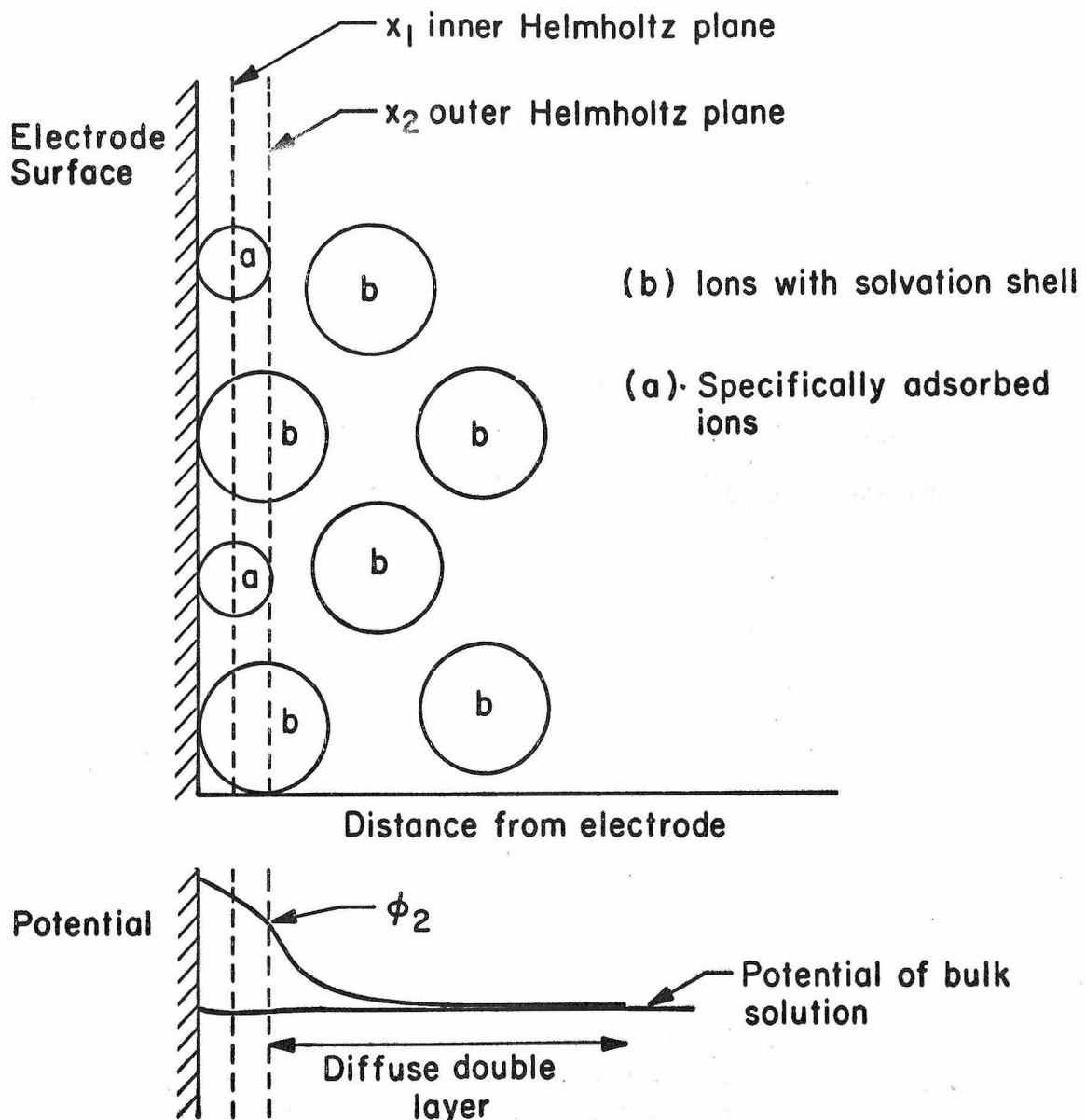
the form of Eq. (7) is now independent of the particular reference electrode used as is the value of the rate constant,  $k_s^a$ , since it refers to the standard potential where forward and reverse rates are equal under standard conditions. The value of  $k_s^a$  is thus truly characteristic of the particular electrode reaction.

Equation (7) is the basic equation that is used to describe a charge transfer reaction; however there are two additional corrections that must be made in the rate equation, which incidentally is the reason that the rate constant,  $k_s^a$ , was defined as the apparent rate constant. These corrections arise from a more detailed model of the interface between the electrode and the solution.

### The Double Layer and Electrode Kinetics

The model that is currently used to describe the electrical double layer which exists at the surface of the electrode was developed independently by Gouy (21) and Chapman (22) and later modified by Stern (23). In the interfacial region at the electrode surface there are solvent molecules and ionic species and since the potential at the metal electrode is in general different from the potential in the bulk of the solution the charged species in solution are either attracted to or repelled from the electrode by the electrical field which exists. Reactants are assumed to be able to approach the electrode surface up to a certain distance which is of the order of the radius of a solvated ion (Fig. 1). This plane of closest approach for solvated ions, at a distance of  $\chi_2$  from the electrode surface, is called the outer Helmholtz plane. Under some conditions, certain ions will lose their associated solvent molecules in the direction of the electrode and approach to a plane situated at a distance of  $\chi_1$  away from the electrode surface. This plane is called the inner Helmholtz plane and the ions which are located at this plane are described as specifically adsorbed. The potential in the double layer region referred to the potential in the bulk of the solution will vary with distance from the electrode and at a distance  $\chi$  from the electrode the potential will be  $\phi$ . Then by introducing a Boltzmann distribution function the concentration of ionic species in the double layer region can be calculated and will be given by the expression:

**Figure 1.** A pictorial representation of the interfacial region near the surface of an electrode.



$$c_X = c_B \exp\left[-\frac{zF}{RT} \phi_X\right].$$

Frumkin (24) was the first to correlate this picture of the double layer with electrode kinetics and demonstrate the expected effects of the double layer conditions on electrode kinetics. He assumed that the electron transfer reaction takes place with the reactants at the outer Helmholtz plane. Therefore two corrections must be made to the Eq. (7) describing the charge transfer reaction. The concentration of charged species at the outer Helmholtz plane will in general be different from their bulk concentrations and will be given by

$$c_{i\chi_2} = c_{iB} \exp\left[-\frac{z_i F}{RT} \phi_2\right] \quad (8a)$$

and also the effective potential, the potential at the outer Helmholtz plane is

$$E_{\text{effect}} = E - \phi_2. \quad (8b)$$

Thus, the corrected kinetic expression then becomes

$$i = nF k_s \left[ [Ox]_B \exp\left(-\frac{z_{Ox} F}{RT} \phi_2\right) \exp\left\{-\frac{\alpha n F}{RT} (E - \phi_2 - E^0)\right\} \right. \\ \left. - [Red]_B \exp\left(-\frac{z_R F}{RT} \phi_2\right) \exp\left\{\frac{(1-\alpha)n F}{RT} (E - \phi_2 - E^0)\right\} \right] \quad (9)$$

$$i = nF k_s \left[ \exp(\alpha n - Z_{ox}) \frac{F}{RT} \phi_2 \right] \left\{ [Ox]_B \exp -\frac{\alpha n F}{RT} (E - E^0) \right. \\ \left. - [Red]_B \exp \frac{(Z_{ox} - n - Z_R)F}{RT} \phi_2 \exp \frac{(1-\alpha)nF}{RT} (E - E^0) \right\}. \quad (10)$$

Furthermore, if  $Z_{ox} = Z_R + n$  this expression becomes

$$i = nF k_s \left[ \exp(\alpha n - Z_{ox}) \frac{F}{RT} \phi_2 \right] \left\{ [Ox]_B \exp -\frac{\alpha n F}{RT} (E - E^0) \right. \\ \left. - [Red]_B \exp \frac{(1-\alpha)nF}{RT} (E - E^0) \right\}. \quad (11)$$

If the apparent standard rate constant,  $k_s^a$ , is defined in the following way,

$$k_s^a \equiv k_s \exp \frac{(\alpha n - Z_{ox})F}{RT} \phi_2$$

Eq. (7) and Eq. (11) are identical.

Since the necessary double layer data are often unavailable, the most frequently reported rate constants are actually only apparent rate constants, uncorrected for double layer contribution.

The potential,  $\phi_2$ , in Eq. (12) is the potential at the outer Helmholtz plane when the electrode potential is that at which the rate constant is being measured. Since  $\phi_2$  is a function of the electrode potential, the apparent rate constants obtained from kinetic experiments will also be potential dependent. If, in addition, the variation of  $\phi_2$  with electrode potential is linear which is often true over limited

potential ranges, a Tafel plot (2),  $\ln i$  vs.  $(E - E^0)$ , will yield values of the transfer coefficient, obtained from the slope, which differ from the real transfer coefficient.

If double layer data are available, the standard, potential-independent rate constant as well as the true transfer coefficient can be obtained. Equation (11) can be rearranged into the following form,

$$\frac{i \exp\left(\frac{Z_{\text{ox}} F}{RT} \phi_2\right)}{\left(1 - \frac{[\text{Red}]_B}{[\text{Ox}]_B} \exp\left[\frac{nF}{RT} (E - E^0)\right]\right)} = [\text{Ox}]_B^{nF} k_s \exp^{-\frac{\alpha nF}{RT} (E - \phi_2 - E^0)} \quad (11a)$$

Now a plot of the logarithm of the left-hand side of Eq. (11a) against  $(E - \phi_2 - E^0)$  will have an intercept proportional to the standard rate constant and a slope proportional to the transfer coefficient.

### The Potential Step Method. Mass Transfer Considerations

The particular form of the kinetic equations that result when mass transfer effects are included vary with the relaxation technique that is used for the kinetic investigation. We will consider the potential step method (4, 25) applied under conditions where convection and migration effects can be ignored so that semi-infinite linear diffusion is the single operative mass transport process. The measured response is either current or its integral, charge. Since we will be assessing the relative merits of charge and current measurement, equations for each case will be given.

In this technique, the potential of the electrode at which the kinetics are to be measured is controlled by a potentiostat which can abruptly change the potential of the electrode and maintain it at any value by supplying the necessary current. Initially, the electrode, a hanging mercury drop of known area immersed in a solution containing only the oxidized half of the redox couple to be studied, is maintained at a potential such that no reaction occurs. The potential of this electrode is then stepped to a value where the charge transfer reaction occurs. Information about the electron transfer rate is obtained by analyzing the resulting time transient of either the current or charge.

The equations that have been derived for both of these cases are as follows:

## A. Current as a function of time (25)

$$i(t) = \kappa \exp(\lambda^2 t) \operatorname{erfc}(\lambda t^{\frac{1}{2}}) + i_{dl}(t) \quad (13)$$

## B. Charge as a function of time (26)

$$Q(t) = \frac{\kappa}{\lambda^2} \left[ \exp(\lambda^2 t) \operatorname{erfc}(\lambda t^{\frac{1}{2}}) + \frac{2 \lambda t^{\frac{1}{2}}}{\pi^{\frac{1}{2}}} - 1 \right] + Q_{dl} \quad (14)$$

where

$$\kappa = nFAC k_s^a \left[ -\frac{\alpha nF}{RT} (E - E^0) \right] \quad (15)$$

$$\lambda = k_s^a \left[ \frac{\exp[-\frac{\alpha nF}{RT} (E - E^0)]}{D_{ox}^{1/2}} + \frac{\exp[\frac{(1-\alpha)nF}{RT} (E - E^0)]}{D_R^{1/2}} \right] \quad (16)$$

$$\operatorname{erfc}(y) \equiv \frac{2}{\pi^{1/2}} \int_y^{\infty} e^{-t^2} dt \quad (27)$$

In the above equations  $i(t)$  and  $Q(t)$  are the total current and charge at a time,  $t$ ,  $i_{dl}(t)$  and  $Q_{dl}(t)$  are the current and charge at any time,  $t$ , involved in the charging of the electrical double layer existing at the electrode,  $A$  is the electrode area, and  $D_{ox}$  and  $D_R$  are the diffusion coefficients of the oxidized and reduced species. Kappa,  $\kappa$ , is the current that would flow if mass transfer of the reactants were very high and is a measure of the intrinsic electron transfer rate. The function,  $\exp(y^2) \operatorname{erfc}(y)$ , accounts for the effects

of mass transfer on current. This function varies from a value of one when its argument is zero to a value of zero when the argument,  $y$ , becomes large. When  $y = 5$ , the function has a value of 0.1107.

Since  $y = \lambda t^{\frac{1}{2}}$ , mass transfer effects become more significant as Lambda,  $\lambda$ , or time become large. Lambda becomes larger as the apparent standard rate constant,  $k_s^a$ , becomes larger, as the absolute value of  $(E - E^0)$  becomes larger, or as the diffusion coefficients,  $D_{ox}$  and  $D_R$ , become smaller. Simply stated, this means that whenever the prevailing rate of electron transfer is sufficiently rapid compared to the rate of diffusion of the reacting species its concentration at the electrode surface will become depleted and the overall rate of the reaction will become controlled by the rate of mass transport to the electrode surface.

**II. Utilization of Statistical Techniques in Electrode  
Kinetics Experiments**

## Statistical Analysis of Kinetic Data

The theoretical equations for the time response of either current or charge (Eqs. (13) and (14)) are non-linear in the parameters to be determined, Kappa, Lambda, and the double layer charging,  $i_{dl}(t)$  or  $Q_{dl}(t)$ . Successive approximation methods must be used to obtain the desired kinetic parameter. The three general methods that are most often employed are linearization using a Taylor series expansion, steepest descent, and Marquardt's compromise (28). For the experiments that were carried out in this research, linearization by Taylor series expansion was chosen and employed. This method has the disadvantage that there is a danger of divergence if the initial estimates for the parameters are too far removed from the final optimal estimates. Fortunately, it was generally possible to obtain sufficiently good initial estimates in the cases studied. The advantage of this method over the alternate methods is that when it does converge it generally converges more rapidly. In addition, this method is less complex mathematically than the others.

The Taylor series expansion method (28, 29) will be illustrated using the equation for the charge measurement variation of the potential step technique. We will assume that the double layer has been charged by the time at which the first measurement is taken so that the charging term may be treated as a constant parameter independent of time. The discussion which follows is also applicable to the current measurement variation of the potential step technique

with only slight modification.

The equation for the charge time response can be written in the following form:

$$Q(t) = \hat{a} + \hat{b} f(\hat{c} t) + \epsilon \quad (17)$$

where  $Q(t)$  is the measured charge at anytime;  $a, b, c$  are the parameters to be determined and the best estimates for them are given by  $\hat{a}, \hat{b}, \hat{c}$ ; and  $\epsilon$  is the error associated with the measurement of the charge. If the initial estimates for the parameters are sufficiently close to the final estimates, the equation can be expanded using a Taylor series expansion neglecting terms that are higher than first order. If the initial estimates for the parameters are  $a^0, b^0, c^0$  and the final estimates are  $\hat{a}, \hat{b}, \hat{c}$  and we let

$$\hat{Q} = Q(\hat{a}, \hat{b}, \hat{c}, t)$$

$$Q^0 = (a^0, b^0, c^0, t)$$

then

$$\hat{Q} = Q^0 + \frac{\partial Q^0}{\partial a} (a - a^0) + \frac{\partial Q^0}{\partial b} (b - b^0) + \frac{\partial Q^0}{\partial c} (c - c^0)$$

if we define

$$Q - Q^0 \equiv y$$

$$a - a^0 \equiv p_1 \quad b - b^0 \equiv p_2 \quad c - c^0 \equiv p_3$$

$$\frac{\partial Q^0}{\partial a} \equiv z_1^0 \quad \frac{\partial Q^0}{\partial b} \equiv z_2^0 \quad \frac{\partial Q^0}{\partial c} \equiv z_3^0$$

$$y \simeq \sum_i p_i z_i^0 + \epsilon. \quad (18)$$

Equation (18) is now in a linear form which is suitable for linear least-squares analysis. The normal equations resulting from this analysis can now be solved for the parameters,  $p_i$ , which are to be estimated. These estimations,  $p_i$ , can be combined with the initial estimates,  $a^0, b^0, c^0$ , to provide improved initial values for another Taylor series expansion. This iterative process is continued until the estimates have converged to the desired degree. Equation (18) was written for one experimental point but in general the experiment consists of  $n$  experimental points which are to be analyzed to provide the best estimates for the parameters. For the general case we can write, using the preceding definitions,

$$Z = \begin{bmatrix} z_{11}^0 & z_{21}^0 & z_{31}^0 \\ z_{12}^0 & z_{22}^0 & z_{32}^0 \\ \vdots & \vdots & \vdots \\ z_{1n}^0 & z_{2n}^0 & z_{3n}^0 \end{bmatrix} \quad P = \begin{bmatrix} p_1 \\ p_2 \\ \vdots \\ p_3 \end{bmatrix}$$

$$Y = \begin{bmatrix} y_1 \\ y_2 \\ \vdots \\ y_n \end{bmatrix} \quad \text{where } Z, Y, \text{ and } P \text{ are matrices}$$

The solution for  $P$ , the parameter estimates, is given by

$$P = (Z' Z)^{-1} Z' Y \quad (19)$$

the form of the above equation is the same as in the linear case since a linear approximation for the theoretical non-linear equation was used.

The most significant difference is that the independent variable matrix,  $Z$ , is a function of the parameters in the non-linear case while with a linear equation the matrix is independent of the parameters which are to be estimated and is a function only of the independent variables. In the linear case when it can be assumed that the variance can be associated with the dependent variables or at least that the variance associated with the dependent variable is very much larger than any variance associated with the independent variables, estimates for the variance associated with the estimated parameters are given by the following equation

$$\text{Var}(p_i) = \nu_{ii} \sigma^2 \quad (20)$$

where  $\sigma^2$  is the variance associated with the dependent variable and  $\nu_{ii}$  are the diagonal elements of the variance-covariance matrix,  $(Z' Z)^{-1}$ . In the linear case the diagonal elements  $\nu_{ii}$  of the variance-covariance matrix are functions only of the independent variable and can be thought of as scale factors which relate the variance of the dependent variable to the estimated variance of the

parameters. Because the variance-covariance matrix in the non-linear case is a function of the parameters to be estimated it will have some variance associated with it as distinguished from the linear case. Thus the estimates obtained for the variance of the parameters estimated will only be approximate and will be lower limits. However, except in cases of extreme non-linearity, the estimates arrived at for the variances of the determined parameters will be good (30).

If we return to the linear case, another use of the variance-covariance matrix can be pointed out. As was stated, the diagonal elements of this matrix can be considered as a set of scale factors which relate the variance of the dependent variable to that of the estimated parameters. These scale factors can be varied by choosing different ranges for the independent variables and thus the estimates for the variance of the parameters can be varied. To relate this to a specific example, if we were to determine the slope of a straight line by sampling at various points along this line, we would expect to be able to determine the slope with more precision with the samples well spaced along the line than if the samples were clustered about one point. For the same variance associated with the dependent variable, the scale factors would be higher for the clustered points than for the well-spaced points so the variance estimates of the slope would be higher in the case with the clustered points. These scale factors, the diagonal elements of the variance-covariance matrix, give an indication of the efficiency of our experimental design. The smaller the scale factors, given a specific level for the variance

of the dependent variable, the smaller the estimated variance of the parameters, or, in other words, the greater the information which we have obtained from the given experiment. The reciprocals of the scale factors are thus proportional to the amount of information which we have obtained by using a given experimental design. In choosing a particular experimental design we would like to maximize the information which we can obtain about the parameters or, equivalently, minimize the variance of these parameters.

If we return again to the non-linear case, the previous discussion is only approximately true because the scale factors are not independent of the parameters estimated. However the diagonal elements of the variance-covariance matrix will give lower limits in estimating the parameter variance and their reciprocals will give upper limits in estimating the information derived about the parameters. Examination of the diagonal elements of the variance-covariance matrix for several experimental designs will enable the experimenter to choose the particular design which will serve to maximize the information about the parameters in which he is interested. This type of approach also enables the experimenter to choose between several experimental techniques, each of which may provide estimates for the parameters in which he is interested.

### Statistics and "Kinetic Information Density"

There has been some discussion (10, 31-33) previously in the literature about the relative merits of current or charge measurement techniques to gain information about electrode kinetic parameters. Various approaches have been taken in the past to try to establish the relative advantages of each method. These previous analyses have reached varying conclusions depending upon the criteria of quality employed. We decided to address the problem by comparing the expected variance of the estimated parameters arising from the two techniques to assess their relative merits.

Before discussing the results of these comparisons the past approaches that have been used and their shortcomings will be pointed out.

It has been asserted (32, 34) that the measurement of charge should be superior to the measurement of current because charge, being the integral of the current retains information about the kinetics of reactions which occurred at all earlier times during the integration. While this is an appealing intuitive argument it would be more powerful and compelling if it could be put in more quantitative terms.

In an attempt to do this Oldham and Osteryoung (10) and, more recently, Osteryoung and Osteryoung (33) have put forward the following ideas: the net response (current or charge) can be thought of as a combined response due to both mass transfer, which is independent of charge transfer kinetics, and charge transfer which is

the rate process of interest. The amount by which the kinetics of charge transfer diminishes the measured response compared to the response that would result from pure diffusion control is a direct measure of the "kinetic information" contained in the response and is called the "kinetic information density". These authors have compared the kinetic information density of charge and current measurement and have concluded that under the usually accessible experimental conditions charge measurement is superior to current measurement. This definition allows the "kinetic information density" to be quantified but there are still some shortcomings to this approach: An ideal, errorless experiment is considered rather than a more realistic experimental situation. The approach taken by Osteryoung and Osteryoung neglects the problem of a realistic appraisal of experimental error. An experiment where current or charge could be measured without error would, by their definition, have the same "kinetic information density" as an experiment where there was a great deal of error in measuring current or charge. Their approach gives the "kinetic information density" of the response for a particular combination of the kinetic parameters and the independent variable while in a actual experiment one obtains and analyzes data for a range of values of the independent variable and the "information density" for that particular experimental design is of more immediate use and importance than the "information density" at one particular point in the experiment. It is also reasonable to expect (because of interaction between data points) that the total amount of

kinetic information would be different than the sum of the kinetic information density at each of the data points.

What follows is an error analysis for the two techniques under consideration. This analysis employs standard, well-known methods (30, 35-37) which, however, have not been directly applied to measurements of electrode kinetics. One is interested in assessing the errors to be expected in the kinetic parameters to be evaluated, arising from the unavoidable errors in the experimental measurement of charge or current. Equation (20) gives the relationship between the variance of the measured response and expected variance of the parameters. In comparing two techniques which estimate the same parameter, the technique which gives the more precise estimate for the parameter is the better technique. If the two techniques have the equal values for the variance of the measured response,  $\sigma^2$ , then the technique which has the smaller diagonal element that relates the variance of the measured response to the variance of the parameter is the better technique.

Since Kappa is the kinetic parameter that is used to determine the standard rate constant a comparison of the estimated variance of Kappa for charge and current measurement will give an indication of the relative merits of the two techniques. Using Eq. (20)

$$\text{Var}(\kappa_Q) = \nu_Q \sigma_Q^2 \quad (21a)$$

$$\text{Var}(\kappa_I) = \nu_I \sigma_I^2 \quad (21b)$$

$$\text{or} \quad \frac{\text{Var}(\kappa_Q)}{\text{Var}(\kappa_I)} = \frac{\nu_Q \sigma_Q^2}{\nu_I \sigma_I^2} \quad (22)$$

where  $\text{Var}(\kappa_Q)$  and  $\text{Var}(\kappa_I)$  are the estimated variances of the parameter Kappa when charge and current are measured,  $\nu_Q$  and  $\nu_I$  are the corresponding diagonal elements of the variance-covariance matrix and  $\sigma_Q^2$  and  $\sigma_I^2$  are the variances of the measured variable, charge and current. The reciprocals of the estimated parameter variances will be proportional to the information obtained by the particular experiment so Eq. (22) can be rewritten:

$$\frac{\text{Inf}(\kappa_Q)}{\text{Inf}(\kappa_I)} = \frac{\nu_I \sigma_I^2}{\nu_Q \sigma_Q^2} \quad (23)$$

where  $\text{Inf}(\kappa_Q)$  and  $\text{Inf}(\kappa_I)$  are measurements of the amount of information about the parameter Kappa that are obtained when measuring charge and current.

To make explicit comparisons between charge and current measurement, the experimental design must be specified. Also since the equations are non-linear particular values for the parameters to be determined must be specified. The values of the parameters and constants chosen for this analysis were selected because they match the corresponding parameters for the electrode reaction that was to be studied,  $\text{Zn}^{+2}/\text{Zn}(\text{Hg})$ . Inasmuch as the standard rate constant and the time were varied over wide ranges, the particular values that were chosen for the constants that arise in the kinetic equations will

affect the results but they will not affect the trends that are apparent in the results nor the conclusions that will be drawn. The diffusion coefficients of the oxidized and reduced species were set equal to  $9 \times 10^{-6}$  moles/cm<sup>3</sup>, and the following constants were assigned values as follows:

$$n = 2$$

$$A = .032 \text{ cm}^2$$

$$C = 1 \times 10^{-6} \text{ moles/cm}^3$$

$$\alpha = 0.2$$

Calculations were made for the standard rate constant equal to  $1 \times 10^{-3}$ ,  $1 \times 10^{-2}$ , and  $1 \times 10^{-1}$  cm/sec. Comparisons were made for experimental designs where the first data point would be taken at times ranging from 10  $\mu$ seconds to 0.1 seconds. The experimental design analyzed assumed fifty equally spaced data points for each comparison and the spacing between data points was made equal to time between the initiation of the experiment and the first-data point. That is, if the first-data point was to be taken at 10  $\mu$ seconds after initiation of the experiment then 50 data points would be taken having a interval between each other of 10  $\mu$ sec. Correspondingly, if 0.1 second was to be the time of the first-data point then the sampling interval was chosen to be 0.1 second. The potential was varied to include values of  $\frac{nF}{RT}(E - E^0)$  of 0, -1, and -2 corresponding to potential steps of 0, 60, and 120 mvolts cathodic of the standard potential. To facilitate comparisons the variances of the measured response,  $\sigma_Q^2$  and  $\sigma_I^2$ ,

Table I. Information (Kappa)

Initial point time msec	Current measurement	Charge measurement	Standard rate constant
0.01	5.18	$4.34 \times 10^{-1}$	$1 \times 10^{-3}$ cm/sec
0.1	4.93	9.13	
1	4.24	$7.17 \times 10^2$	
10	2.73	$4.24 \times 10^4$	
100	$8.69 \times 10^{-1}$	$1.09 \times 10^6$	
			$1 \times 10^{-2}$ cm/sec
0.01	4.24	$7.17 \times 10^{-2}$	
0.1	2.73	4.24	
1	$8.69 \times 10^{-1}$	$1.09 \times 10^2$	
10	$7.67 \times 10^{-2}$	$7.61 \times 10^2$	
100	$9.77 \times 10^{-4}$	$1.76 \times 10^3$	
			$1 \times 10^{-1}$ cm/sec
0.01	$8.69 \times 10^{-1}$	$1.09 \times 10^{-2}$	
0.1	$7.67 \times 10^{-2}$	$7.61 \times 10^{-2}$	
1	$9.77 \times 10^{-4}$	$1.76 \times 10^{-1}$	
10	$1.99 \times 10^{-6}$	$2.36 \times 10^{-1}$	
100	$2.93 \times 10^{-9}$	$2.60 \times 10^{-1}$	

Table II. Information (Kappa)

Initial point time msec	Current measurement	Charge measurement	Standard rate constant
			$1 \times 10^{-3}$ cm/sec
0.01	5.13	$1.93 \times 10^{-1}$	
0.1	4.80	8.47	
1	3.92	$6.52 \times 10^2$	
10	2.19	$3.27 \times 10^4$	
100	$5.23 \times 10^{-1}$	$6.06 \times 10^5$	
			$1 \times 10^{-2}$ cm/sec
0.01	3.92	$6.52 \times 10^{-2}$	
0.1	2.19	3.27	
1	$5.23 \times 10^{-1}$	$6.06 \times 10^1$	
10	$2.90 \times 10^{-2}$	$2.97 \times 10^2$	
100	$2.07 \times 10^{-4}$	$5.65 \times 10^2$	
			$1 \times 10^{-1}$ cm/sec
0.01	$5.23 \times 10^{-1}$	$6.06 \times 10^{-3}$	
0.1	$2.90 \times 10^{-2}$	$2.97 \times 10^{-2}$	
1	$2.07 \times 10^{-4}$	$5.65 \times 10^{-2}$	
10	$3.15 \times 10^{-7}$	$7.02 \times 10^{-2}$	
100	$1.88 \times 10^{-9}$	$6.85 \times 10^{-2}$	

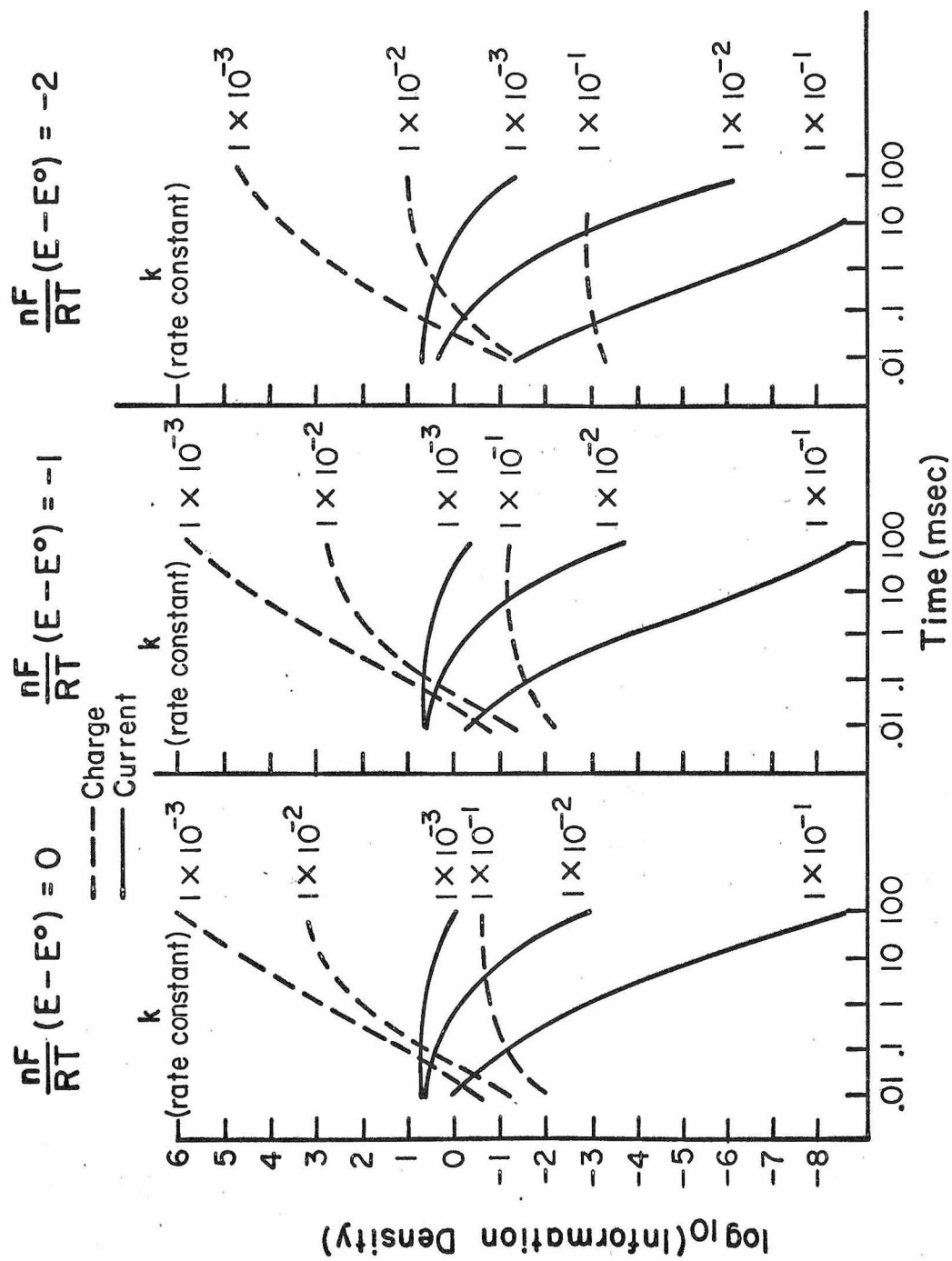
$$\alpha = .2 \quad \frac{nF}{RT} (E - E^0) = -1$$

Table III. Information (Kappa)

Initial point time msec	Current measurement	Charge measurement	Standard rate constant
			$1 \times 10^{-3}$ cm/sec
0.01	4.87	$8.71 \times 10^{-2}$	
0.1	4.09	6.86	
1	2.46	$3.76 \times 10^2$	
10	$6.84 \times 10^{-1}$	$8.27 \times 10^3$	
100	$4.83 \times 10^{-2}$	$4.82 \times 10^4$	
			$1 \times 10^{-2}$ cm/sec
0.01	2.46	$3.76 \times 10^{-2}$	
0.1	$6.84 \times 10^{-1}$	$8.27 \times 10^{-1}$	
1	$4.83 \times 10^{-2}$	4.82	
10	$4.64 \times 10^{-4}$	$1.01 \times 10^1$	
100	$7.95 \times 10^{-7}$	$1.29 \times 10^1$	
			$1 \times 10^{-1}$ cm/sec
0.01	$4.83 \times 10^{-2}$	$4.82 \times 10^{-4}$	
0.1	$4.64 \times 10^{-4}$	$1.01 \times 10^{-3}$	
1	$7.95 \times 10^{-7}$	$1.29 \times 10^{-3}$	
10	$3.45 \times 10^{-9}$	$1.42 \times 10^{-3}$	
100	$2.06 \times 10^{-8}$	$7.39 \times 10^{-4}$	

$$\alpha = .2 \quad \frac{nF}{RT}(E - E^0) = -2$$

**Figure 2.** Reciprocals of the variance-covariance matrix diagonal elements relating to the parameter, Kappa, in kinetic experiments using the potential step method as functions of time and potential for current and charge measurement.



were assumed to be equal to one and the kinetic information tabulated is equal to the reciprocal of the appropriate element of the variance-covariance matrices for charge and current measurements. If  $\sigma_Q^2$  and  $\sigma_I^2$  are equal to each other but not equal to one the ratio will still be the same as the ratio of the tabulated values. If  $\sigma_Q^2$  and  $\sigma_I^2$  are not equal, then they must be included to form the correct information ratio.

The particular experimental design for the spacing between data points was chosen to contrast with results of Osteryoung and Osteryoung (33). Since Osteryoung and Osteryoung make their determination of "kinetic information density" by using in effect a one point sample, an experimental design that would correspond more closely to their situation would be samples where the spacing between points was small and where this spacing was kept constant regardless of the time of the initial sample. If this type of design is chosen, results similar to those of Osteryoung and Osteryoung are obtained; that is, the kinetic information rapidly decreases with increasing time for both charge and current measurement with charge measurement being superior to current measurement for all but the shortest experiment times. In contrast, the results that are shown in Tables I, II, and III and Fig. 2 indicate that for a constant value of  $\sigma_Q^2$  an experimental design where the data points are not closely clustered will still give good estimates of the kinetic parameters at long experimental times. It can be seen in Fig. 2 that charge measurement would be expected to give more precise results, i. e., more "kinetic

information", than would current measurement at experimental times equal to or greater than about 100  $\mu$ seconds. The actual crossover time varies but is generally in this neighborhood. Also the higher the intrinsic charge transfer rate,  $k_s$ , or the effective charge transfer rate, reflected in effect of potential on the information, the smaller the amount of kinetic information available for a given level of variance of the measured response. Although at short enough experimental times current measurement would appear to be the technique of choice other considerations enter in which prevent making a clear cut distinction. At experimental times that are early enough to be in a region where current measurement would be superior, the assumption that was made about the charging of the double layer being complete by the time the first experimental point was taken may no longer be valid. Thus, in most typical experimental situations charge measurement should be superior to current measurement for evaluating kinetic parameters.

Although the same conclusion was reached by Osteryoung and Osteryoung on the basis of their analysis, the type of analysis outlined here reveals more of the major importance of experimental design on the information that can be obtained from kinetic experiments. The definition of "kinetic information density" used by Osteryoung and Osteryoung can not account for the factor of experimental design for two reasons: first of all it does not treat the measured response and secondly and more importantly their definition refers to the kinetic information at only a single isolated

Table IV. Reciprocals of Variance-Covariance Diagonal Elements for Kinetic Parameters for Current Measurement and for Charge Measurement

-E (mV) vs. SCE	Current Measurement		Charge Measurement	
	Kappa	Lambda	Kappa	Lambda
940	$3.64 \times 10^{-1}$	$1.22 \times 10^{-5}$	4.07	$1.57 \times 10^{-4}$
960	1.04	$2.35 \times 10^{-4}$	$1.42 \times 10^1$	$3.63 \times 10^{-3}$
980	2.72	$2.54 \times 10^{-3}$	$4.56 \times 10^1$	$4.57 \times 10^{-2}$
990	3.34	$5.41 \times 10^{-3}$	$5.86 \times 10^1$	$1.00 \times 10^{-1}$
1000	3.57	$8.94 \times 10^{-3}$	$6.36 \times 10^1$	$1.67 \times 10^{-1}$
1010	3.60	$1.24 \times 10^{-2}$	$6.43 \times 10^1$	$2.32 \times 10^{-1}$
1020	3.42	$1.66 \times 10^{-2}$	$6.03 \times 10^1$	$3.09 \times 10^{-1}$
1030	3.04	$1.99 \times 10^{-2}$	$5.22 \times 10^1$	$3.63 \times 10^{-1}$
1040	2.67	$2.22 \times 10^{-2}$	$4.46 \times 10^1$	$3.98 \times 10^{-1}$
1050	2.17	$2.41 \times 10^{-2}$	$3.47 \times 10^1$	$4.19 \times 10^{-1}$
1060	1.81	$2.46 \times 10^{-2}$	$2.78 \times 10^1$	$4.17 \times 10^{-1}$
1080	1.03	$2.10 \times 10^{-2}$	$1.41 \times 10^1$	$3.24 \times 10^{-1}$
1100	$5.16 \times 10^{-1}$	$1.45 \times 10^{-2}$	6.16	$1.99 \times 10^{-1}$
1120	$2.21 \times 10^{-1}$	$8.15 \times 10^{-3}$	2.27	$9.64 \times 10^{-2}$
1140	$7.14 \times 10^{-2}$	$3.17 \times 10^{-3}$	$6.17 \times 10^{-1}$	$3.10 \times 10^{-2}$
1160	$2.00 \times 10^{-2}$	$1.03 \times 10^{-3}$	$1.46 \times 10^{-1}$	$8.31 \times 10^{-3}$
1180	$4.39 \times 10^{-3}$	$2.54 \times 10^{-4}$	$2.71 \times 10^{-2}$	$1.68 \times 10^{-3}$
1200	$8.16 \times 10^{-4}$	$5.10 \times 10^{-5}$	$4.26 \times 10^{-3}$	$2.77 \times 10^{-4}$

point and therefore is not applicable to the experimental situation as it is normally encountered.

The previous discussion illustrated the comparison of kinetic information obtained for a wide variation of time and rate constant. To provide a more quantitative comparison that reflects more closely the actual conditions under which the kinetic experiments herein described were performed, values of the kinetic parameters obtained from actual kinetic experiments were used to calculate the amount of kinetic information available from charge and current measurements under the particular experimental conditions that were employed. For these experiments one hundred experimental points were used and a sample was taken every 400  $\mu$ seconds.

Table IV and Figs. 3 and 4 show the reciprocals of the diagonal elements of the variance-covariance matrices for the kinetic parameters, Kappa and Lambda. These results show very strikingly the effect of potential on the amount of kinetic information that can be obtained from measurements at various potentials with a given level of variance of the dependent variable. Figures 3 and 4 compare charge measurement versus current measurement and show that charge measurement should yield superior results over the entire potential range. Also a comparison of Fig. 3 with Fig. 4 indicates that since Kappa can be obtained with more precision, i.e., higher information, than Lambda, it is preferable to obtain the rate constant from Kappa.

Table V and Fig. 5 have been included to indicate more clearly the need for better precision at higher charge transfer rates. This

**Figure 3.** Potential dependence of the variance-covariance matrix elements relating to the kinetic parameter, Kappa.

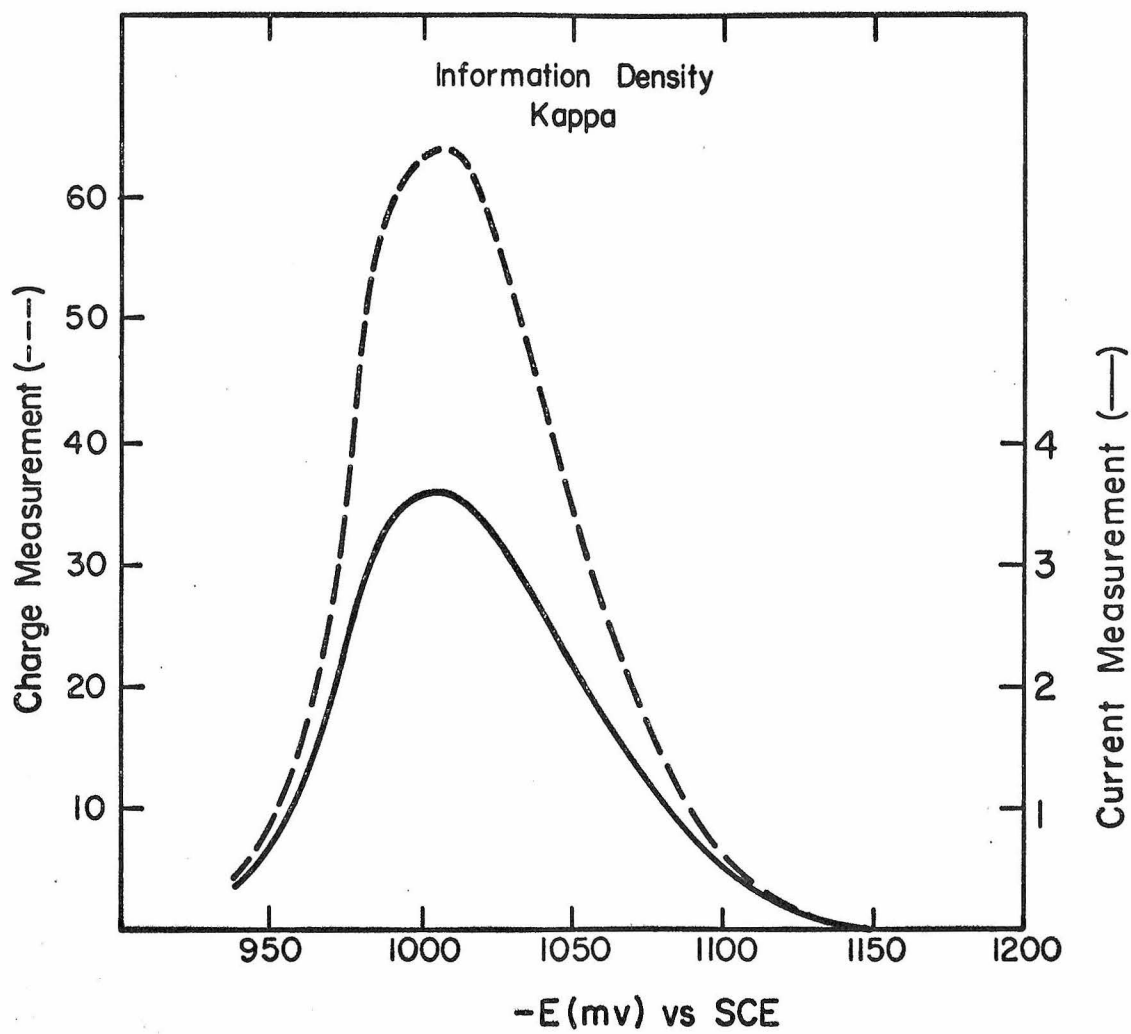


**Figure 4.** Potential dependence of the variance-covariance matrix elements relating to the kinetic parameter, Lambda.

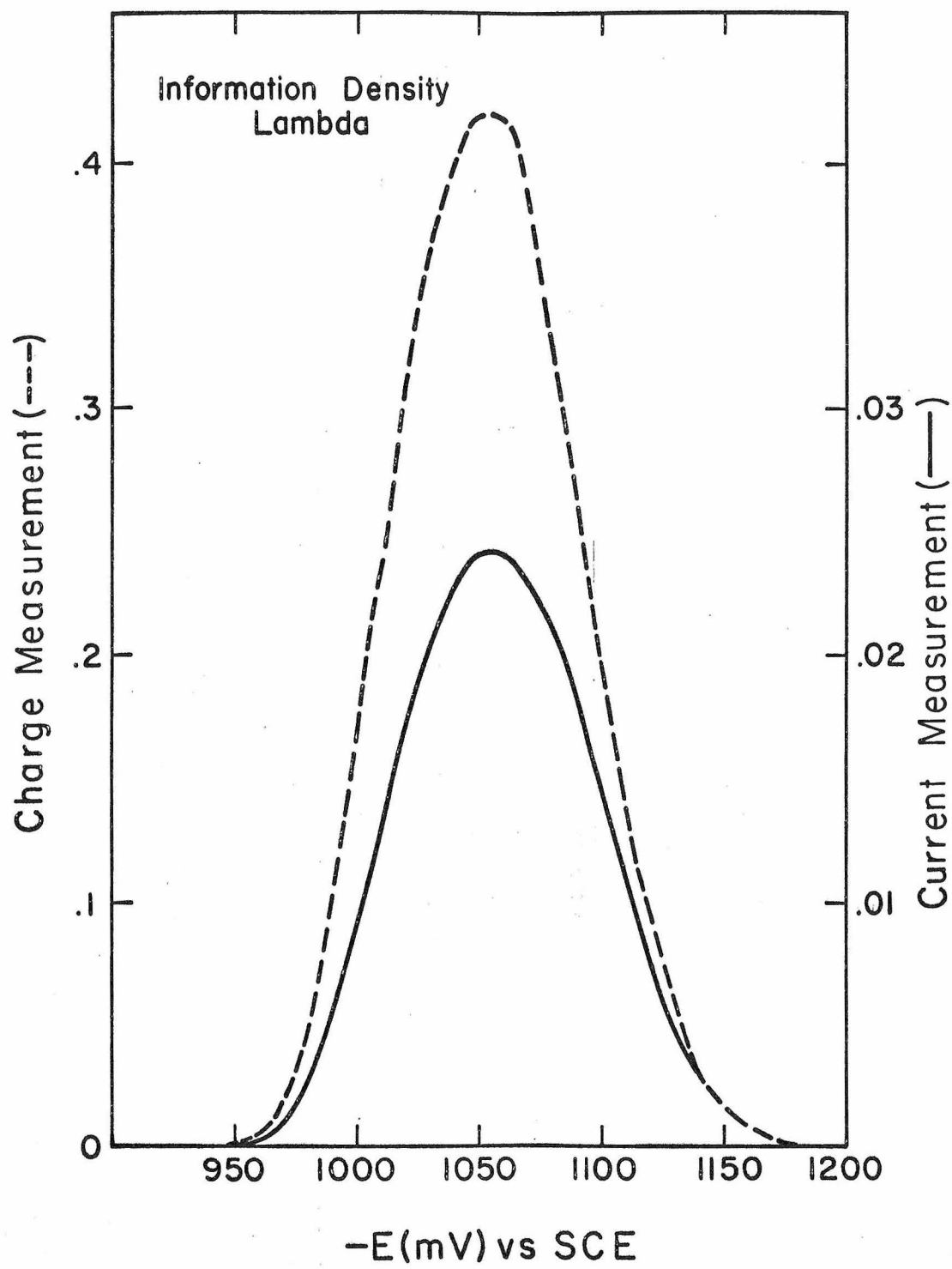


Table V. Logarithm of Variance-Covariance Element of  
Kappa for Charge and Current Measurement

-E (mV) potential vs. SCE	Charge	Current
940	1.221	2.269
960	0.678	1.813
980	0.170	1.396
990	0.063	1.306
1000	0*	1.256
1010	0.023	1.274
1020	0.050	1.295
1030	0.113	1.347
1040	0.180	1.403
1050	0.289	1.494
1060	0.386	1.572
1080	0.681	1.817
1100	1.040	2.118
1120	1.473	2.485
1140	2.040	2.976
1160	2.666	3.529
1180	3.397	4.188
1200	4.201	4.916

\* Arbitrary scale set to zero at -1000 mV for Kappa obtained by charge. To change to absolute scale this value is -1.830.

**Figure 5.** Relative expected imprecision of Kappa for charge and current measurement as functions of potential.

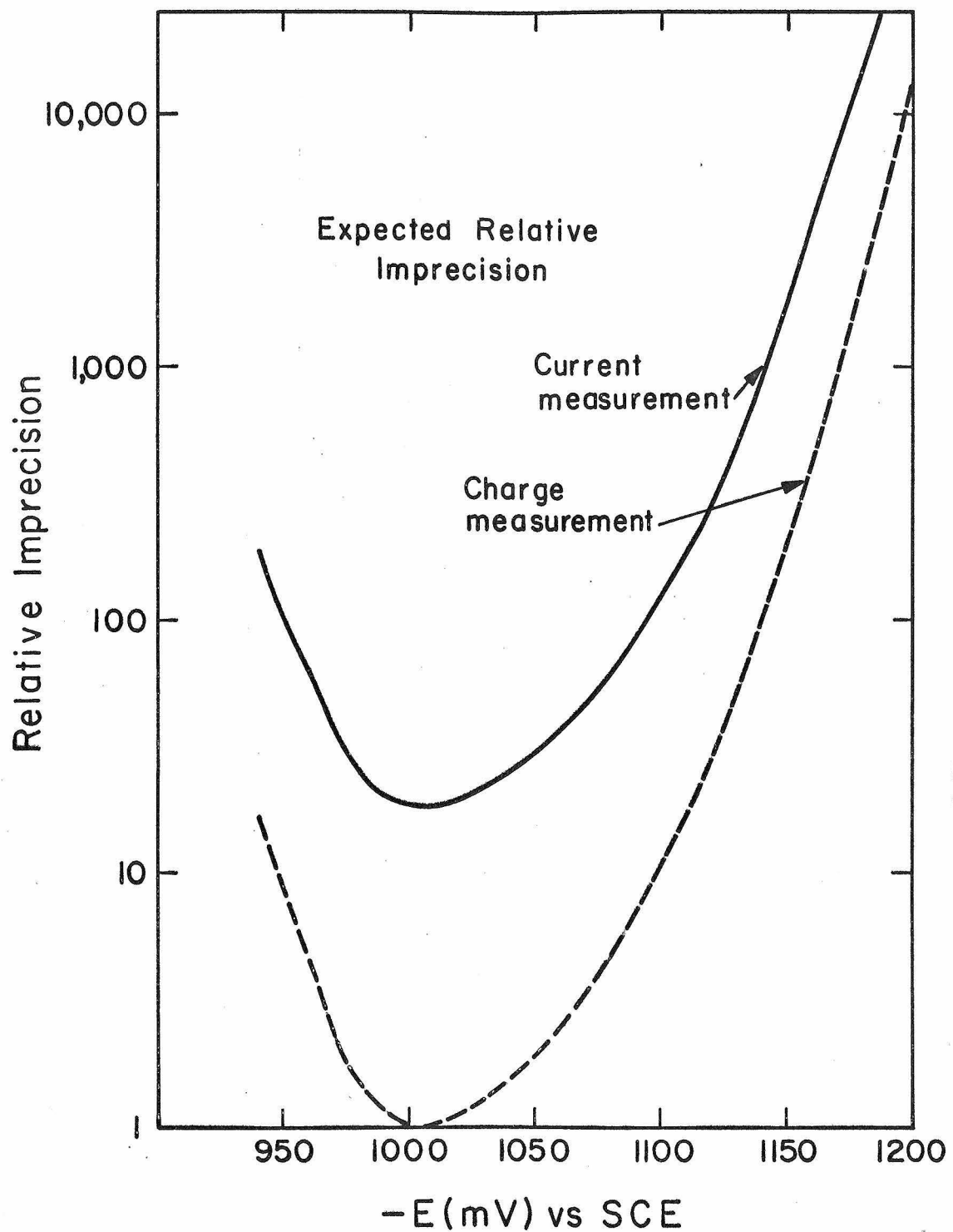


table and figure show the increased precision with which it is necessary to measure the dependent variable in order to maintain a constant level of variance for the kinetic parameter Kappa. The level of variance for Kappa at -1000 mv vs. S. C. E. for charge measurement was chosen as the desired level. The numbers in Table V are logarithms of the ratio of variance of the dependent variable at -1000 mv vs. S. C. E. to the variance of the dependent variable at various other potentials which are necessary to maintain a constant variance for Kappa. Thus for charge measurements, the charge must be measured approximately ten times as accurately at -1100 mv vs. S. C. E. to obtain the same level of variance in Kappa as was obtained at -1000 mv vs. S. C. E. Likewise the current must be measured about 18 times more accurately at -1000 mv vs. S. C. E. to obtain comparable results to charge measurements at the same potentials.

III. Acquisition and Analysis of Kinetic Data by  
a Digital Computer

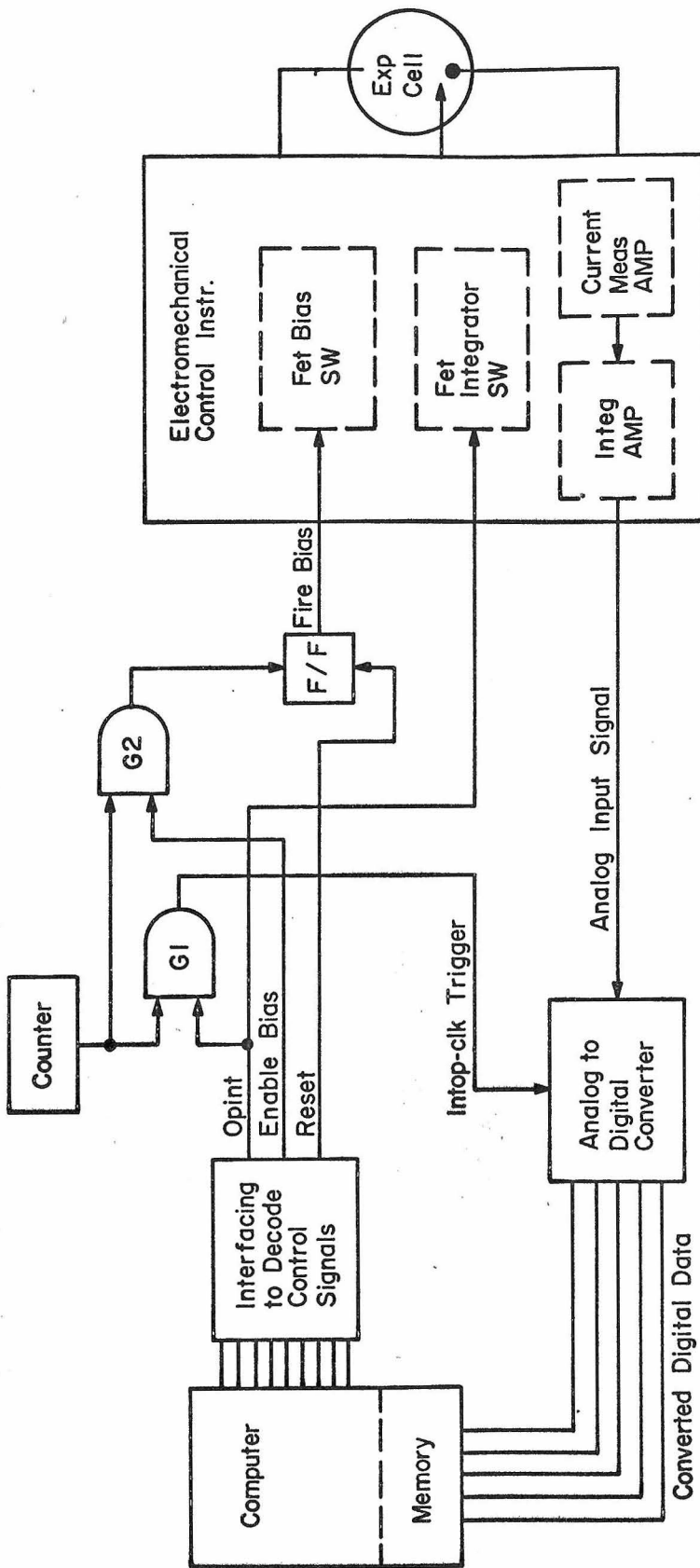
## Computerized Data Acquisition and Analysis System

The components of the computerized data acquisition and analysis system are shown in a block diagram in Fig. 6. These components will be described and then the interconnections that are necessary to provide a useful system for data acquisition and analysis will be detailed.

The potentiostat used in the experiments is part of a general purpose electrochemical instrument which has previously been described (38). The potentiostat uses operational amplifiers (Philbrick, Boston, Mass.) to control the potential of a hanging mercury drop electrode at a value that is preselected. Potentiometers are used to vary the potential and field effect transistor (FET) switches are used to step the potential from one value to another. The current flowing at the hanging mercury drop is measured using an operational amplifier connected as a current measuring amplifier. The output of the current measuring amplifier is connected to an operational amplifier designed as an integrator. The output of this amplifier is a voltage analog signal which is proportional to the amount of charge that has passed at the hanging mercury drop electrode since the initiation of the integration which is accomplished by unshorting the feedback capacitor of the operational amplifier. Switching is accomplished by using another FET switch. This instrument is the part of the system which controls the actual perturbation applied to electrode and acts as a transducer and signal shaper of the

**Figure 6.** A block diagram of the computerized data acquisition and analysis system showing necessary interconnections.

Block Diagram of Computer System



response signal (an analog voltage) that results from the applied perturbation.

The digital computer is a Model 660-5 computer manufactured by Scientific Control Corporation of Dallas, Texas. This computer has a basic cycle time of 5  $\mu$ seconds and a memory size of 4096 words (4 K), each word containing 24 bits.

The memory is expandable to 32K and is directly accessible by the computer. The computer has three main 24 bit registers; an arithmetic register, an extended arithmetic register which is used for most mathematical calculations, and an index register which is extremely useful when doing repetitive sequences of instructions. The command structure is well designed; it contains about 50 basic instructions several of which are very useful for control and data-acquisition purposes. Typewriter and paper tape are the principal means of communication between the experimenter and computer. However there are four breakpoint switches which can be set by the operator and tested by the computer in order to alter the flow of the program execution. External priority interrupts (2 channels) have been provided and may be enabled by setting a switch or by program commands. Control signals for external devices as well as lines for input and output of data are readily available at connectors on the computer. There are 12 control signal lines available which enable the generation of up to  $2^{12}$  or 2048 separate control signals. These control signals are available as 5  $\mu$ second pulses. The input and output of data to and from the computer takes a minimum of 15  $\mu$ sec

(3 cycles) and usually more since the computer waits until transfer of data is complete before proceeding with the execution of the next command.

The analog voltage signal from the general purpose electro-chemical instrument is sampled and converted into digital form by a Model 8500-MS Analog to Digital Converter (ADC) with a Type 38400 Sample and Hold (Preston Scientific Corp., Anaheim, Calif.). This ADC has a maximum through-put rate for data of 13  $\mu$ sec per 12 bit data word, a range of  $\pm 5$  volts full scale, a converted data word of 11 bits plus a sign bit. The specified accuracy is 1/2 of the least significant bit (1.22 mV). The logic levels (0 volt, +8 volts) and numerical format (twos complement) are the same as is used by the digital computer. The ADC was designed to begin conversion upon receiving an external timing signal and to provide a signal indicating that the data have been converted and are ready to be read.

Because the computer clock used for internal timing is a free running multivibrator whose frequency is temperature dependent an external accurate clock was necessary. A Systron Donner Corp. (Concord, Calif.) Model 1033 Counter with a Model 1944 present plug-in is used to provide timing signals. This counter is accurate to at least one part in  $10^7$  and can supply pulses whose repetition rate are adjustable over a range of from 10  $\mu$ seconds to 10 seconds. The counter provides signals, which after appropriate gating, to be discussed next, control the sampling rate for data acquisition by trigger data conversion in the ADC.

The basic components which have just been described were interconnected to achieve the necessary synchronization and control required for accurate and reproducible data acquisition. Although the interfacing has been designed to be applicable to several electrochemical techniques (38-40), the timing and synchronization features that are available will be discussed only in reference to experiments in electrode reaction kinetics described in this thesis. The computer system is designed to perform the following sequence of operations:

- i) Open the integrator to enable it to commence measuring charge and detect any offset that exists;
- ii) Apply a bias potential to the operational amplifier to step the electrode potential to the desired value;
- iii) Provide for the sampling of data points at accurately known times;
- iv) Reset the system to its initial configuration after the required number of data points have been obtained.

Because actions that are taken by the system must occur at times which are accurately known, the control functions, opening the integrator, sampling data, stepping the bias, are gated with clock pulses and are accomplished using FET switches. Since the FET switches are very fast, typically of the order of  $10^{-7}$  sec, all actions occur on the first-clock pulse after the computer command has been given. Since the clock pulses can be counted either by counting the number of data points read by the computer or by counting the number of external priority interrupts which the computer has received,

synchronization and accurate timing can be maintained. Figure 7 indicates the signals that are used and the particular sequence in which they are employed to perform a typical kinetic experiment. Before the initiation of the experiment the interfacing is reset, the integrator is shorted and the potential is at its initial value. Counter pulses are available at the output of the counter at all times, however the control signals that are necessary to open the gates for the counter pulses are absent.

To commence the experiment, the operator engages the run switch on the computer. This initiates the execution of the kinetic program which causes the following actions to take place. A control signal from the computer opens the gate which enables the next clock pulse to open the integrator and initiate data conversion in the ADC. Succeeding clock pulses will cause the ADC to convert the analog input signal to a digital number. Several points are sampled (the precise number is selected by the operator) to obtain an accurate baseline reading for the integrator. After the desired number of points have been read into the computer, the computer sends out another control signal which opens the gate which enables the potential to be stepped. On the first clock pulse after the control signal, in addition to the previously mentioned actions, the FET switch controlling the stepping of the potential is fired. Succeeding clock pulses again trigger the conversion of data by the ADC. When the desired number of experimental points (again preselected by the operator) have been obtained the computer sends out control signals which cause the gates

**Figure 7.** Time sequence diagram depicting signals and events occurring in a typical kinetic experiment.

Figure 7 (cont'd)

### Signals

The interfacing which decodes the control signals converts them to levels which are used to control the gates.

**OPINT** -- "open the integrator" this control signal fires the FET switch which opens the integrator and opens G1 for the passage of counter pulses which subsequently cause data conversion at the ADC.

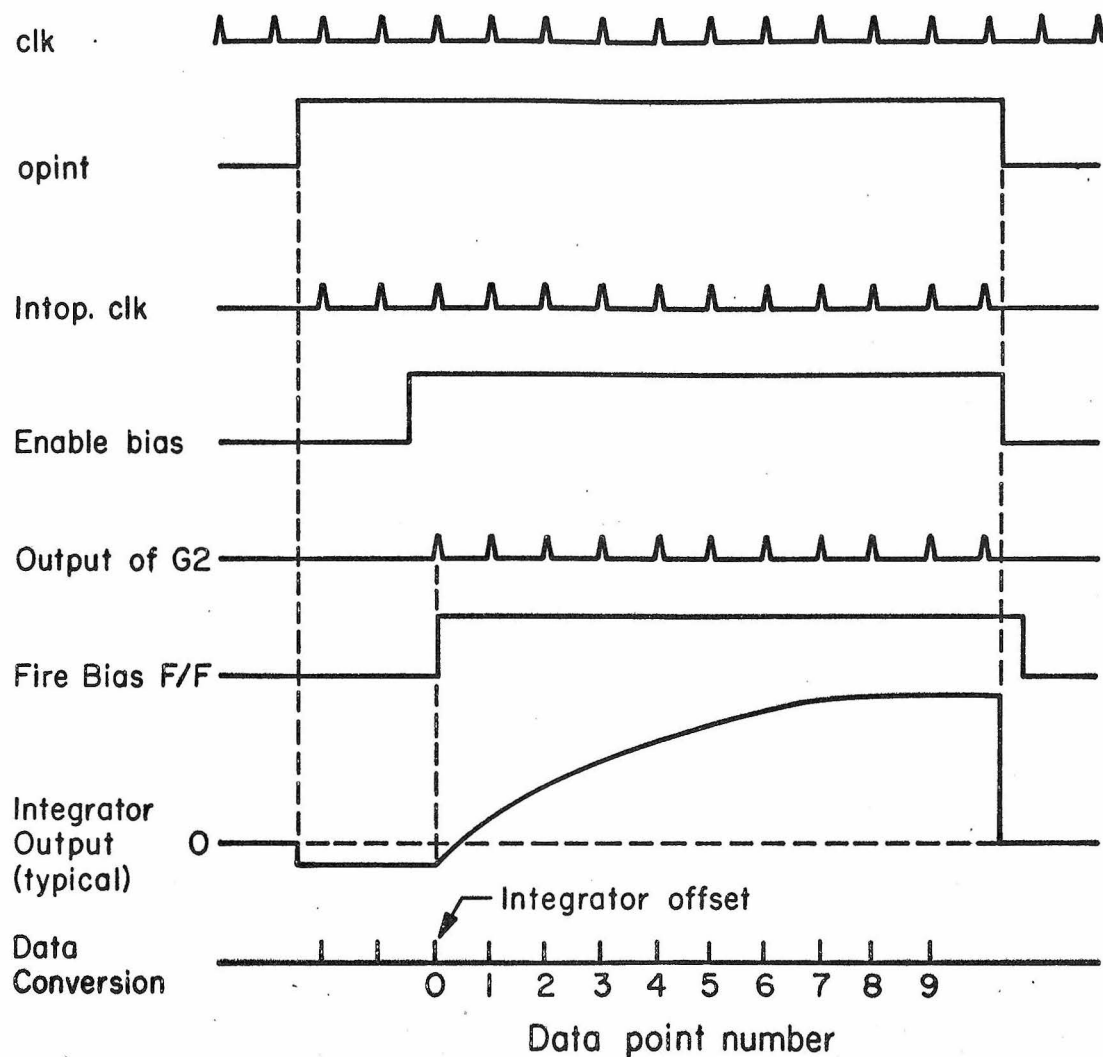
**Intop.clk** -- This signal is the output of G1 and, as described above, triggers the ADC.

**Enable bias** -- This control signal opens G2 for the passage of counter pulses. The first counter pulse after the enable bias signal sets the F/F.

**Fire bias** -- This signal appears at the output of F/F and fires the FET switch which steps the bias.

**Reset** -- This signal resets the F/F to its initial condition.

## Timing Diagram



to be closed and the conditions returned to their initial states.

A gated pulse from the counter initiates data conversion by the ADC every time a pulse is received by the ADC, the integrator is opened and the potential is stepped when the first gated counter pulse is received. However, they must remain in these states until the experiment has been completed. To accomplish this, the respective gated counter pulses are used to trigger bistable devices (flip-flops, F/F) which maintain their state until reset by the appropriate reset signals.

IV. Investigation of the  $Zn^{+2}/Zn(Hg)$  Electrode Reaction in  
1 F  $NaNO_3$ , 1 F  $NaClO_4$ , and 1 F  $NaCl$

### Experimental Conditions

The solutions that were used for the measurements of the kinetics of the reduction of zinc(II) ion at a mercury electrode were always 1 F in supporting electrolyte, either  $\text{NaNO}_3$ ,  $\text{NaClO}_4$  or  $\text{NaCl}$ , and either 1 mF or .5 mF in zinc ion. The electrode, a hanging mercury drop, was renewed after every experimental run.

Each of the experiments was performed in the following manner: The mercury electrode was initially potentiostated at -800 mV vs. S. C. E. where no faradaic reaction occurred. The potential was then stepped to a value where the faradaic reaction occurred and the resulting charge-time response was recorded using the computer system previously described. The potential to which the electrode was stepped was varied over the range of -1000 mV to -1200 mV vs. S. C. E. Data points were obtained every  $500 \mu \text{sec}$  after the initiation of the experiment until one hundred points had been obtained (50 msec). To improve the precision of the data, ensemble averaging was employed. Ensemble averaging was advantageous not only because it improved precision but also because it cut down overall experimental time. Although each set of data was obtained in 50 msec the analysis of the data using non-linear least squares took several minutes. Thus when several sets of data, generally four, were combined and only the ensemble average analyzed quite a bit of time could be saved. Ensemble averages of four runs were chosen because, when the number of runs is a power of two, the computer could take the

average merely by shifting numbers contained in a register the appropriate number of times. When the noise that appears with the desired signal is not correlated with the signal, ensemble averaging can be expected to improve the signal-to-noise ratio proportional to the square root of the number of runs that are averaged (41).

To compare ensemble averaging to the normal procedure, four sets of data were analyzed separately and parameter estimates were obtained. Then the ensemble average of the data sets was analyzed. The results showed that the estimate of the square root of the variance of the dependent variable was decreased by a factor of about two while the estimates for the kinetic parameters obtained from the data showed no apparent bias as a result of ensemble averaging.

The data obtained from the kinetic experiment were analyzed using the three parameter non-linear least-squares analysis discussed on page 22. Normally the first five data points were deleted from the analysis because there was evidence that instrumental response was affecting the validity of the data obtained at these early times. It must be remembered that the model employed assumes instantaneous charging of the double layer whereas in fact the charging of the double layer is not instantaneous. The first few data points showed a tendency to be low as would be expected if the charging of the double layer, which is assumed to be completed, is still occurring. When the first five points were deleted from the analysis the experimental data followed the fitted response quite well. Several features indicated that a satisfactory fit was being obtained: A visual inspection of the

residuals showed no trends except as mentioned for the first five points. There was no systematic deviation between the actual and fitted data and the residuals were all the same order of size over the entire range of the data that were analyzed. This visual inspection of residuals was made only in some of the experiments. However a test for randomness of the residuals (2) was used for every analysis performed. In view of the fact that a slight time correlation of the residuals might be expected to exist, the results obtained from the randomness test are probably best viewed as semi-quantitative or qualitative indicators of the adequacy of the analysis. Generally this test indicated that the residuals were random and the analysis satisfactory. Visual inspection of the residuals in several experiments, where the randomness test indicated that the residuals were more non-random than would be normally expected, revealed no gross systematic deviations of the residuals and in fact the fit obtained appeared to be satisfactory.

A third indication of the adequacy of the analysis was obtained by comparing the estimates for the variance of the dependent variable obtained from the analysis of the data to estimates obtained from instrumental considerations. To obtain an estimate of the variance of the dependent variable it was assumed that the precision of the measurement of the dependent variable in any single experiment was limited by the resolution of the analog to digital converter (A. D. C.) that was used. The accuracy of the A. D. C. as specified by the manufacturer is 1/2 of the least significant bit. If we take the value

of one bit (2.44 millivolts) as a realistic estimate of the precision of the A. D. C., the expected value of the standard error of the dependent variable can be obtained. Since the dependent variable measured was charge in units of  $\mu$ coulombs, the scale factors of the operational amplifiers which were used to provide an analog signal proportional to charge must be given. The formula for the conversion of the analog voltage to charge is given as follows:

$$Q(\mu C) = \frac{RC}{R_M} * 10^6 * V$$

where  $R_M$  is the value (ohm) of the resistor used in the current measuring amplifier,  $RC$  is the time constant (sec) of the resistor and capacitor used in the integrating amplifier, and  $V$  is the analog voltage signal in volts. Table VI gives the results obtained at several selected potentials. Each analysis was an ensemble average of four runs and the estimate of the standard error of the dependent variable is obtained by taking the square root of the estimated variance of the dependent variable which is obtained by dividing the sum of the squared residuals by the appropriate degrees of freedom ( $N-P$ ) where  $N$  is the number of points analyzed and  $P$  is the number of parameters estimated by the analysis. The equality of the measured estimate for the variance of the dependent variable and the calculated estimate of the variance can be tested by taking the ratio of the measured estimate to the calculated estimate and comparing this ratio to a Chi square distribution having  $N-P$  degrees of freedom.

Table VI

$$RC = 10^{-4} \text{ sec}^{-1} \quad n = 4 \quad \sigma_v = 2.44 \times 10^{-3} \text{ volts}$$

$-E_f$ vs. SCE	$R_M$ (ohms)	$\sigma_{\text{Calc.}}$	$\sigma_{\text{Exp.}}$	$\frac{\hat{\sigma}^2}{\sigma^2}$
-1010	500	$2.44 \times 10^{-4}$	$2.21 \times 10^{-4}$	.841
			2.49	1.041
			2.76	1.279
1030			2.01	.678
			2.59	1.127
			2.12	.755
1060	200	$6.10 \times 10^{-4}$	4.69	.591
			5.02	.677
			4.01	.432
1080			5.55	.828
			6.27	1.056

For 90 D. F.  $\frac{\hat{\sigma}^2}{\sigma^2} < 1.257$  95%

$$\sigma_Q^{\text{calc.}} = \frac{(RC)(10^6)}{(R_M)(\sqrt{n})} * \sigma_v$$

For a confidence level of .05, a Chi square distribution with 90 degrees of freedom gives a value of 1.257 (3). This means that if the two estimates of the variance are equal the value of their ratio will exceed 1.257 only about 5% of the time. As can be seen from table the value of the variance of the dependent variable obtained from the analyzed data conforms well with the estimate calculated from instrumental considerations. This is a further indication that the data conform to the model used and are being fitted to the model satisfactorily.

### Experimental Results

For each of the final potentials at which kinetic measurements were made at least four separate experiments were performed, each of which consisted of an ensemble average of four sets of data. The results of these experiments are listed in Tables VII-XII. In these tables precision estimates are given only for the parameter Kappa, since this parameter will be the principal one used to obtain values for the rate constant. However the error levels are comparable for the other two parameters, Lambda and double layer charge,  $Q_{dl}$ . The precision limits that are listed are the 95% confidence limits obtained from calculations using the values of Kappa obtained for the separate experiments.

Although the precision of the results obtained for a given experiment consisting of an ensemble average of four sets of data was limited by the precision of the A. D. C., the variability of the results obtained under nominally the same experimental conditions was significantly greater. The likely reason for this is that although care was taken to reproduce the experimental conditions as closely as possible over a longer period of time some of the unavoidable variability of the experimental conditions caused corresponding changes in the results that were obtained. Such factors as slight variations in temperature or small drifts in potential cause corresponding variations in the results obtained. The results shown in Tables VII-XII and Figs. 8, 9, 10 were obtained from experiments which were

Table VII

1 F NaClO <sub>4</sub>	1 mF Zn <sup>++</sup>		
-E <sub>f</sub> vs. SCE (mv)	$\kappa * 10^2$ (mA)	$\lambda$ (msec <sup>-1</sup> )	$Q_{dl} * 10^1$ ( $\mu$ C)
980	1.695 ± .044	.105	1.04
990	2.109 ± .013	.085	1.10
1000	2.536 ± .016	.074	1.16
1010	3.044 ± .018	.074	1.20
1020	3.675 ± .040	.081	1.25
1030	4.384 ± .044	.091	1.29
1040	5.301 ± .106	.107	1.35
1050	6.294 ± .035	.126	1.38
1060	7.445 ± .084	.148	1.42
1080	10.86 ± .07	.211	1.52
1100	15.75 ± .22	.304	1.59
1120	22.16 ± .59	.430	1.65
1140	31.65 ± .31	.612	1.72
1160	44.98 ± .83	.867	1.79
1180	63.86 ± .79	1.23	1.89
1200	90.27 ± 4.28	1.73	1.98

Table VIII

.5 mF  $Zn^{+2}$  1 F  $NaClO_4$

$-E_f$ vs. SCE (mv)	$\kappa * 10^2$ (mA)	$\lambda$ ( $msec^{-1}$ )	$Q_{dl} * 10^1$ ( $\mu C$ )
980	.876 $\pm$ .013	.104	1.06
990	1.066 $\pm$ .018	.082	1.11
1000	1.273 $\pm$ .050	.072	1.16
1010	1.524 $\pm$ .011	.074	1.22
1020	1.839 $\pm$ .033	.080	1.27
1030	2.216 $\pm$ .022	.092	1.32
1040	2.611 $\pm$ .050	.106	1.38
1050	3.232 $\pm$ .029	.129	1.43
1060	3.814 $\pm$ .050	.151	1.46
1080	5.516 $\pm$ .051	.218	1.56
1100	7.923 $\pm$ .167	.308	1.65
1120	11.30 $\pm$ .12	.438	1.74
1140	16.28 $\pm$ .22	.630	1.82
1160	22.87 $\pm$ .29	.886	1.92
1180	32.88 $\pm$ .51	1.26	2.00
1200	46.83 $\pm$ 3.45	1.79	2.11

Table IX

	1 mF Zn <sup>+2</sup>	1 F NaNO <sub>3</sub>	
-E <sub>f</sub> vs. SCE (mv)	$\kappa * 10^2$ (mA)	$\lambda$ msec <sup>-1</sup>	$Q_{dl} * 10^{+1}$ ( $\mu$ C)
970	1.311 ± .009	.169	.98
980	1.603 ± .077	.117	1.02
990	2.010 ± .020	.088	1.08
1000	2.418 ± .042	.076	1.12
1010	2.940 ± .050	.074	1.17
1020	3.581 ± .042	.080	1.23
1030	4.259 ± .073	.090	1.28
1040	5.055 ± .097	.104	1.32
1060	7.176 ± .059	.144	1.41
1080	10.18 ± .32	.203	1.50
1100	14.24 ± .18	.280	1.62
1120	19.86 ± .53	.391	1.67

Table X

		.5 mF Zn <sup>+2</sup>	1 F NaNO <sub>3</sub>	
-E <sub>f</sub> vs. SCE (mv)		$\kappa * 10^2$ (mA)	$\lambda$ (msec <sup>-1</sup> )	$Q_{dl} * 10^{+1}$ ( $\mu$ C)
970		.664 ± .030	.165	.98
980		.857 ± .024	.115	1.04
990		1.054 ± .038	.088	1.09
1000		1.279 ± .024	.080	1.14
1010		1.541 ± .024	.078	1.20
1020		1.841 ± .016	.082	1.25
1030		2.201 ± .004	.092	1.31
1040		2.635 ± .028	.106	1.35
1050		3.066 ± .050	.121	1.40
1060		3.665 ± .027	.145	1.44
1080		5.241 ± .074	.204	1.54
1100		7.458 ± .046	.290	1.63

Table XI

	1 mF Zn <sup>2+</sup>	1 F NaCl	
-E <sub>f</sub> vs. SCE (mv)	$\kappa * 10^2$ (mA)	$\lambda$ (msec <sup>-1</sup> )	$Q_{dl} * 10^{+1}$ ( $\mu$ C)
980	1.776 ± .028	.194	.97
990	2.408 ± .055	.149	1.02
1000	3.191 ± .064	.122	1.08
1010	4.091 ± .106	.119	1.12
1020	5.227 ± .053	.126	1.17
1030	6.379 ± .059	.138	1.23
1040	7.772 ± .064	.161	1.26
1050	9.798 ± .716	.202	1.31
1060	11.09 ± .07	.222	1.37
1080	16.06 ± .37	.312	1.43
1100	22.33 ± 2.22	.437	1.53

Table XII

		.5 mF Zn <sup>+2</sup>	1 F NaCl	
-E <sub>f</sub> vs. SCE (mv)		$\kappa * 10^2$ (mA)	$\lambda$ (msec <sup>-1</sup> )	$Q_{dl} * 10^1$ ( $\mu$ C)
970		.677 ± .024	.278	.93
980		.961 ± .087	.199	.98
990		1.292 ± .042	.155	1.03
1000		1.671 ± .037	.132	1.08
1010		2.081 ± .016	.121	1.13
1020		2.550 ± .084	.127	1.18
1030		3.285 ± .029	.144	1.24
1040		3.886 ± .040	.162	1.27
1060		5.673 ± .151	.230	1.37
1080		7.812 ± .296	.312	1.47
1100		10.61 ± .50	.419	1.59
1120		14.25 ± .93	.563	1.70
1140		18.48 ± .18	.717	1.82

**Figure 8.** Experimentally obtained results for the double layer charging parameter,  $Q_{dl}$ , for the  $Zn^{+2}/Zn(Hg)$  electrode reaction in 1  $\underline{F}$   $NaNO_3$ , 1  $\underline{F}$   $NaClO_4$ , and 1  $\underline{F}$   $NaCl$  supporting electrolytes.

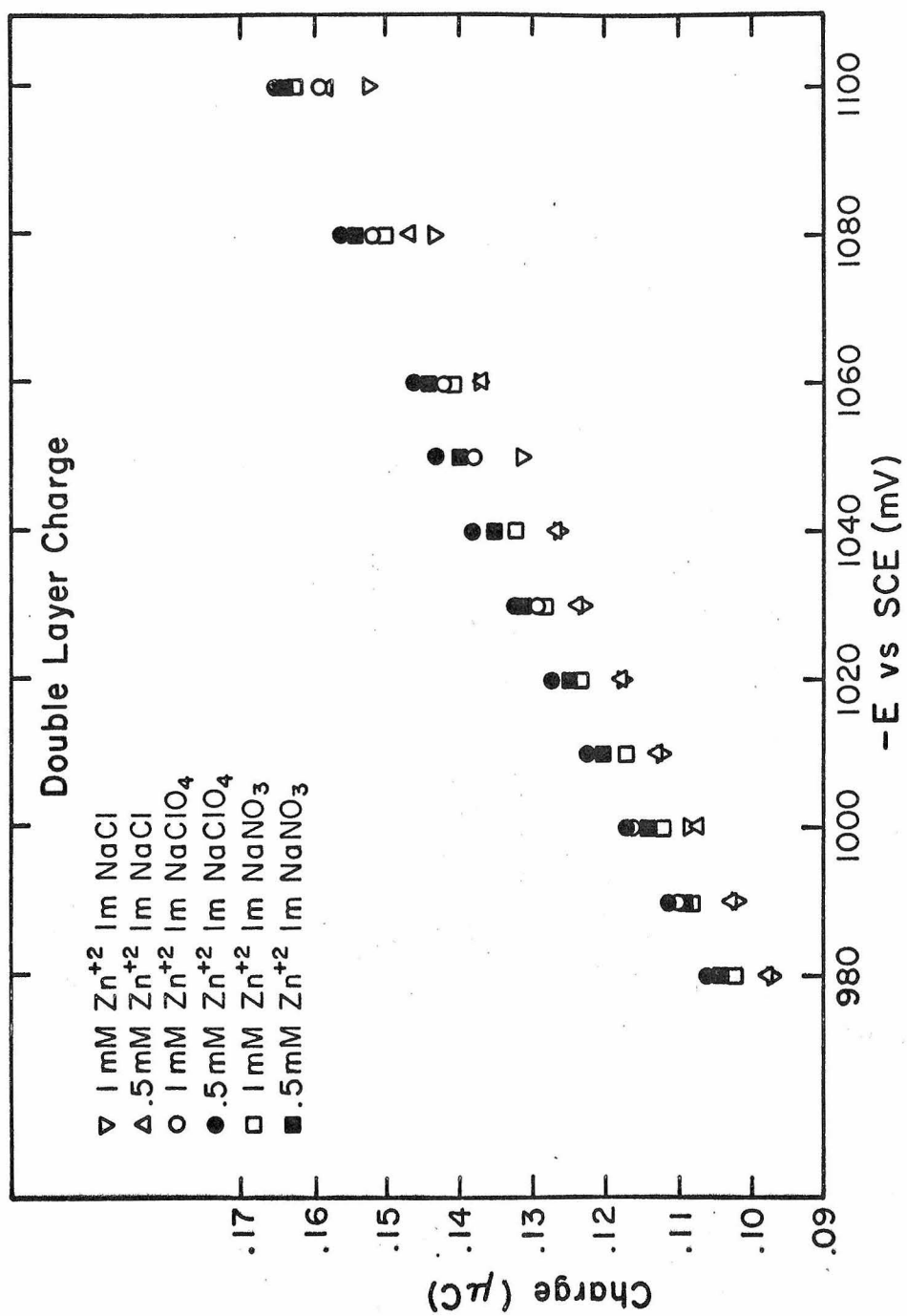


**Figure 9.** Experimentally obtained results for the kinetic parameter,  $\lambda$ , for the  $\text{Zn}^{+2}/\text{Zn}(\text{Hg})$  electrode reaction in  $1 \text{ F NaNO}_3$ ,  $1 \text{ F NaClO}_4$ , and  $1 \text{ F NaCl}$  supporting electrolytes.

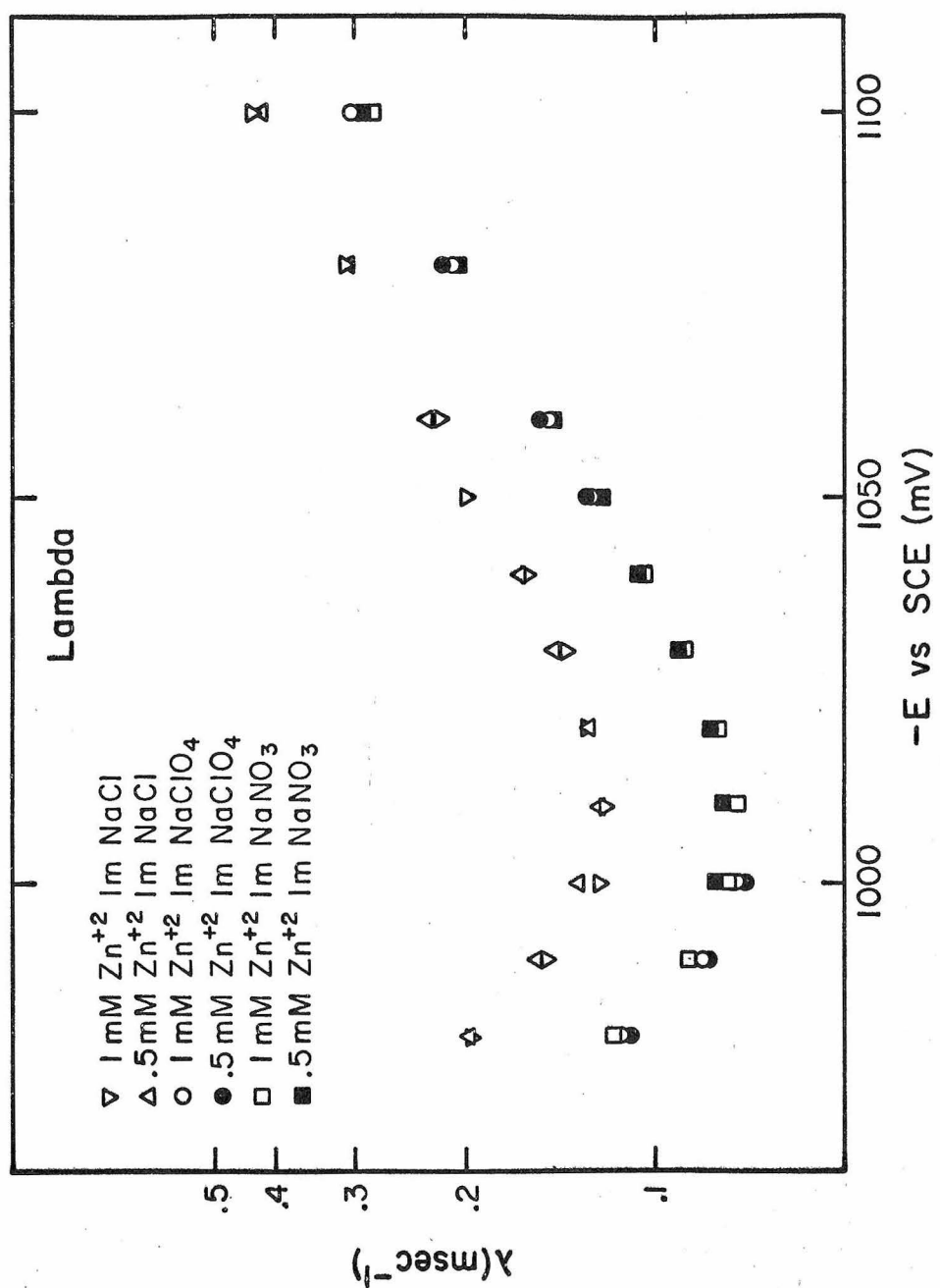
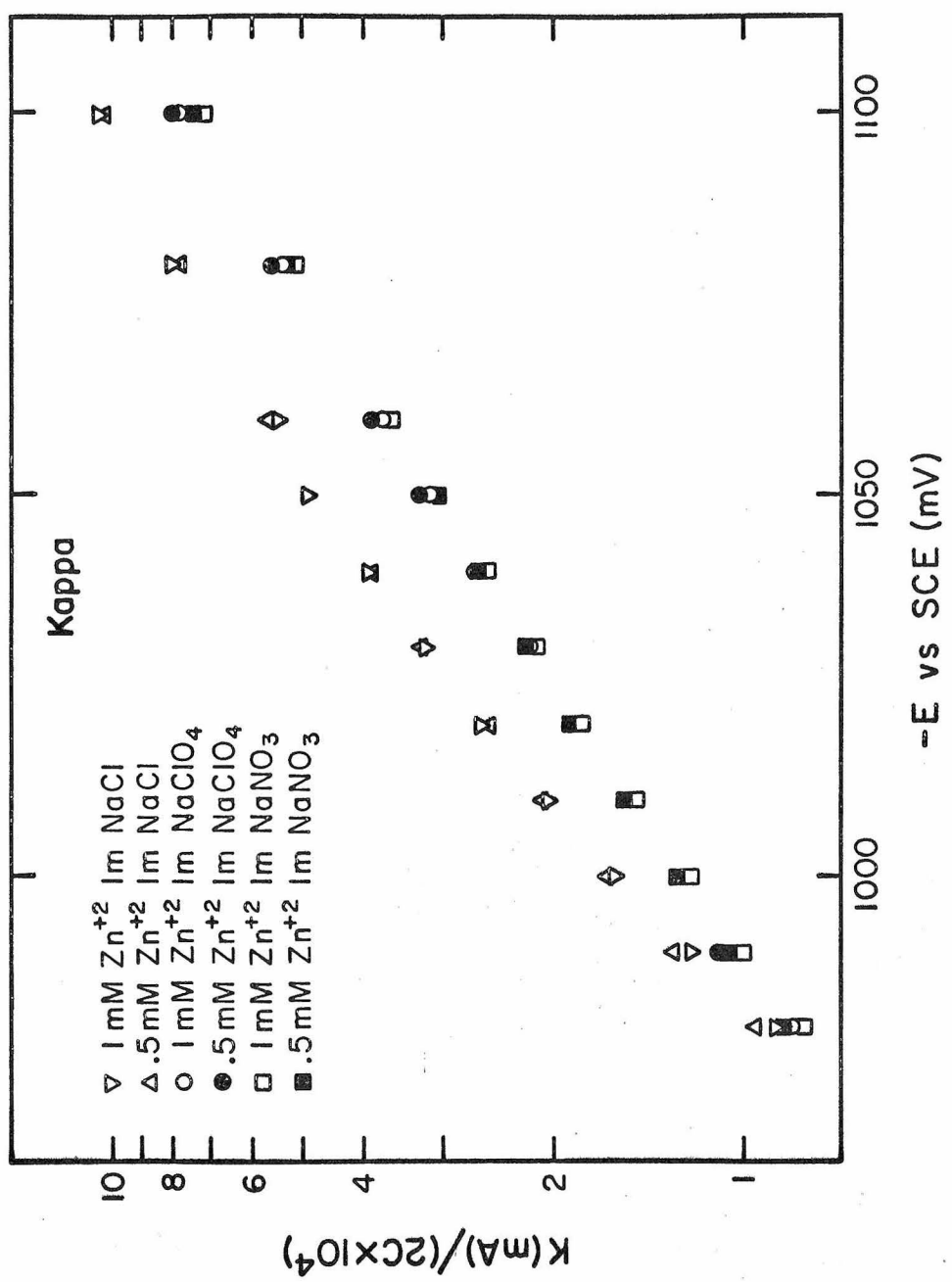


**Figure 10.** Experimentally obtained results for the kinetic parameter,  $\kappa$ , normalized for  $Zn^{+2}$  concentration, for the  $Zn^{+2}/Zn(Hg)$  electrode reaction in  $1 \text{ F NaNO}_3$ ,  $1 \text{ F NaClO}_4$ , and  $1 \text{ F NaCl}$  supporting electrolytes.



carried out over a relatively long period of time in an effort to eliminate any biases that may have been introduced by particular short term variations. The precision limits which are listed reflect the long-term variability. The relative precision of the parameters, as measured by dividing the 95% confidence limits by the parameters were 3% or less except at the extremes of the potential ranges reported where the precision became worse as would be expected from the previous discussion of information density.

Before examining the values obtained for the parameter Kappa in more detail, a brief examination of the other parameters will be undertaken to point out some general indications of the quality of the results.

Turning first to an examination of the results obtained for Lambda, this parameter (Eq. (16)) should be independent of the concentration of zinc ion and where the absolute value of  $(E - E^0)$  is large, i. e., the final potential is sufficiently removed from the standard potential, a plot of the logarithm of Lambda against  $(E - E^0)$  should to a first approximation be a straight line. The conditions that are necessary for this plot to be a straight line are first, one of the terms containing the potential must become negligible with respect to the other and second, the variation of the potential at the outer Helmholtz plane,  $\phi_2$ -potential, with a variation in overall potential must be constant or zero.

If the double layer effects are the same for each of the electrolytes, the values obtained for Lambda should give a direct indication

of the rate constants. Figure 9 shows that the results obtained in supporting electrolytes of  $\text{NaNO}_3$  and  $\text{NaClO}_4$  are very similar. For a supporting electrolyte of  $\text{NaCl}$ , however, there appears to be an enhancement of the rate constant which is well outside of experimental error. Since there is evidence of complexation of zinc in chloride media (14, 44), a direct comparison of the values of Lambda is not strictly valid. Complexation of the zinc by chloride should cause a smaller double layer enhancement than occurs in noncomplexing media with a consequent lowering of the apparent rate. Since the opposite effect is observed, the conclusion that the rate constant in chloride is larger than in nitrate or perchlorate is strongly indicated. A more quantitative discussion of this effect will be deferred until the parameter Kappa is examined.

One final point can be made with reference to the internal consistency of the results by comparing corresponding plots of  $\ln \lambda$  and  $\ln \kappa$  against potential (Figs. 9 and 10). In the potential range negative of the standard potential where the  $\ln \lambda$  plot is linear, the slopes of the  $\ln \lambda$  and  $\ln \kappa$  plots must be equal. The fact that the observed slopes (Fig. 9) are equal is a further indication of internal consistency of the results and of the adequacy of the analysis.

The double layer charging values obtained are slightly harder to compare. The concentrations of zinc that were used are such they have a negligible effect on the  $\phi_2$  potential (15). Therefore the results obtained in each of the supporting electrolytes should be

independent of the zinc concentration. The results shown in Fig. 8 appear to exhibit a slight trend in which lower values of  $Q_{dl}$  occur at the higher concentrations of zinc, especially at potentials that are far from the standard potential. However, this difference is within experimental error which is about 3% and is in the direction to be expected if the potentiostat does not compensate completely for solution resistance (45).

A comparison between the different supporting electrolytes is difficult to make in other than qualitative terms. However the double layer conditions at the mercury electrode for perchlorate and nitrate media can be expected to be very similar at sufficiently negative potentials and should result in values of the double layer charging parameter that are also similar. Chloride media could reasonably be expected to show different values than perchlorate or nitrate since there are indications that there is slight adsorption of the chloride ion at potentials that were used in the kinetic experiments (46).

The parameter Kappa, Eq. (15), is directly proportional to the concentration of zinc and to the apparent rate constant. In Fig. 10, a plot of  $\log \text{Kappa}$  vs. potential, the values of Kappa have been normalized with respect to concentration to enhance the comparison between the supporting electrolytes used. As has been indicated previously in the discussion of Lambda, the rates appear to be the same in perchlorate and nitrate but higher in chloride media.

To make a more quantitative comparison of the rates in the various supporting electrolytes and to obtain actual numerical values of the rate constants, it is necessary to have data about the double layer. Particularly necessary are the values of the potential at the outer Helmholtz plane,  $\phi_2$ , for given values of the overall potential. Kappa,  $\kappa$ , is defined as follows (26)

$$\kappa = nFAC k_S \exp \left[ (\alpha n - z) \frac{E}{RT} \phi_2 \right] \exp \left[ - \frac{\alpha n F}{RT} (E - E^0) \right] \quad (15)$$

When the necessary  $\phi_2$  data are available, a plot of  $(\ln \kappa + \frac{zF}{RT} \phi_2)$ , versus  $(E - \phi_2 - E^0)$  will yield a straight line, whose slope is proportional to alpha,  $\alpha$ , and whose intercept is proportional to the standard rate constant. The other parameter which is necessary in addition to the  $\phi_2$  data is the charge on the oxidized species,  $z$ .

As a first approximation, it will be assumed that the supporting electrolytes used exhibit negligible adsorption over the potential range in which the kinetic measurements were undertaken. To the extent that this assumption is true the double layer in the various electrolytes will be identical and will be the same as the double layer in 1 F NaF where adsorption is known to be absent (47). Values of  $\phi_2$  as a function of potential have been tabulated by Russell (49) for various concentrations of NaF including 1 F. These values were used and where necessary interpolated to provide values of  $\phi_2$  for potentials which were used in the kinetic experiments (Table XIII). The value of the charge on the oxidized species was assumed to be

Table XIII

Potential -E (mV) <u>vs.</u> S. C. E.	$\phi_2$ (1 F NaF) -E (mV)
940	40.6
950	41.1
960	41.7
970	42.2
980	42.6
990	43.2
1000	43.6
1010	44.1
1020	44.6
1030	45.0
1040	45.6
1050	46.0
1060	46.5
1080	47.6
1100	48.5
1120	49.5
1140	50.5
1160	51.5
1180	52.4
1200	53.4

two in nitrate and perchlorate supporting electrolytes since no measurable complexation (48) of zinc takes place in these electrolytes. In the case of chloride media complexation of zinc is known to occur and has been measured by Sillen and co-workers and by Sluyters (14, 44). The values that Sluyters obtained for the formation constants of the zinc chloride complexes are consistent with those obtained by Sillen and co-workers, however only the values obtained by Sluyters are directly applicable to these kinetic studies since they were obtained in 1 F chloride. Sluyters (14) detected only the mono-chloro complex in 1 F chloride and found a formation constant of 0.45. Using this formation constant the average value of the charge of the oxidized species is found to be 1.69 in 1 F NaCl and this value was used when making the double layer correlations in chloride media. A linear least-squares fit of  $(\ln \kappa + \frac{ZF}{RT} \phi_2)$  versus  $(E - \phi_2 - E^0)$  was made of the data for all of the supporting electrolytes. In chloride the data were fit using both 1.69 and 2 as values for the charge of the oxidized species. The results are shown in Table XIV. For a given electrolyte, the rates obtained at the two concentrations of zinc generally agree to within 3% and the variation of rates between nitrate and perchlorate electrolytes is about the same. The difference between chloride and the other two electrolytes is much larger even when the charge of the oxidized species is taken as two. When complexation of the zinc in chloride is taken into account this difference is further magnified.

If we now examine the assumption that adsorption of the supporting electrolyte can be neglected, it is known (50, 51) that in this

Table XIV  
Standard Rate Constants

$Zn^{+2}(mF)$	$\kappa_O$ (ma)	$\alpha$	$k_s$ (cm/sec)
$NaClO_4$			
.5	$8.27 \times 10^{-4}$	.20	$2.68 \times 10^{-4}$
1	$1.63 \times 10^{-3}$	.20	$2.64 \times 10^{-4}$
$NaNO_3$			
.5	$8.14 \times 10^{-4}$	.19	$2.64 \times 10^{-4}$
1	$1.56 \times 10^{-3}$	.19	$2.52 \times 10^{-4}$
$NaCl (z = 2)$			
.5	$1.24 \times 10^{-3}$		$4.02 \times 10^{-4}$
1	$2.51 \times 10^{-3}$		$4.07 \times 10^{-4}$
$NaCl (z = 1.69)$			
.5	$1.99 \times 10^{-3}$	.22	$6.45 \times 10^{-4}$
1	$4.04 \times 10^{-3}$	.24	$6.54 \times 10^{-4}$

potential range this assumption is correct for nitrate and perchlorate. For chloride, however, there is some adsorption even in the potential range where the zinc reaction was studied (46). The adsorption is larger the less negative the potential in this range. If we take the worst case and consider a potential near  $-1000$  mV vs. SCE for which there is data readily available, we can estimate the error caused by the assumption of negligible adsorption. Sluyters et al. (14) have found that at a potential of approximately  $-1010$  vs. SCE the amount of adsorbed chloride in  $1 \text{ F}$  chloride is about  $0.5 \mu\text{C}$  and the corresponding  $\phi_2$  potential is  $-46$  mV. Using the interpolated data from Russell the value of  $\phi_2$  at this overall potential is  $-44$  mV and the discrepancy between the two is  $2$  mV. This difference will be the maximum difference since at more negative potentials the adsorption of chloride decreases to zero at which point  $\phi_2$  will be the same as NaF.

It is possible to determine approximately the effect of the error in  $\phi_2$  upon the rate constant by using the Law of Propagation of Errors (52). If we take the logarithm of Eq. (15) then for small changes in  $\phi_2$  assuming  $(E - E^0)$  and Kappa to be constant we obtain:

$$\left| \frac{\Delta k_s}{k_s} \right| \approx \left| \left( \frac{(\alpha n - 2)F}{RT} \Delta \phi_2 \right) \right| .$$

If we take  $\alpha = .2$ ,  $n = 2$ , and  $z = 2$  or  $z = 1.69$  we obtain

$$\frac{\Delta k_s}{k_s} = .06 \Delta \phi_2 \quad z = 2$$

$$\frac{\Delta k_s}{k_s} = .05 \Delta \phi_2 \quad z = 1.69$$

Thus for an error of 2 mV in  $\phi_2$  one can expect a relative percentage error of 10-12% in the standard rate constant for the worst case.

This error in the rate constant is rather large, however it should be pointed out that the values of  $\phi_2$  obtained from Russell are also not error-free and probably themselves have an imprecision of about 1 mV. Also, even if worst cases are assumed throughout, the experimental values of the standard rate constant in chloride in comparison to those in nitrate or perchlorate are greater than can be explained simply by an error in the value of  $\phi_2$ .

Most previous workers have evaluated "apparent" rather than "standard" rate constants (2) by neglecting the effect of the double layer on the observed rates. Instead of Eq. (15), an equation such as (15a) was used to evaluate  $k_a$ .

$$\kappa = nFAC k_a \exp \left( -\frac{\alpha nF}{RT} (E - E^0) \right)$$

The resulting apparent rate constants,  $k_a$ , appears to be potential dependent because the double layer effect on the rate is included in the apparent rate constant. Nevertheless, comparison of the rate constants obtained in this study with those obtained by previous workers is readily possible because apparent rate constants can be calculated from standard rate constants through the use of the necessary  $\phi_2$  data. A point by point calculation of the apparent rate

constant corresponding to each potential is needed and depends upon the availability of appropriate  $\phi_2$  data. Under some experimental conditions the variation of  $\phi_2$  with overall potential is very nearly linear. For this special case there exists a simpler way of obtaining apparent rate constants than the above point by point calculation. A plot of  $\ln \kappa$  vs.  $(E - E^0)$  is linear under these circumstances with an intercept which is proportional to the apparent rate constant. An examination of Table XIII reveals that the variation of  $\phi_2$  with overall potential is approximately linear so that apparent rate constants can be readily obtained from the kinetic data which were used to calculate the standard rate constants. A least-squares fit of  $\ln \kappa$  vs.  $(E - E^0)$  was performed on the kinetic data and the results are shown in Table XV. The error limits which are given in this table are the 95% confidence limits calculated using the appropriate number of degrees of freedom.

Table XV  
Apparent Rate Constant

$Zn^{+2}(mF)$	$\kappa_a$ (mA)	$k_s^a$ (cm/sec)
$NaClO_4$		
.5	$1.27 \pm .02 \times 10^{-2}$	$4.11 \pm .05 \times 10^{-3}$
1	$2.50 \pm .06 \times 10^{-2}$	$4.05 \pm .08 \times 10^{-3}$
$NaNO_3$		
.5	$1.27 \pm .02 \times 10^{-2}$	$4.11 \pm .07 \times 10^{-3}$
1	$2.43 \pm .07 \times 10^{-2}$	$3.93 \pm .10 \times 10^{-3}$
$NaCl (z = 2)$		
.5	$1.64 \pm .10 \times 10^{-2}$	$5.31 \pm .14 \times 10^{-3}$
1	$3.16 \pm .28 \times 10^{-2}$	$5.12 \pm .42 \times 10^{-3}$

### Discussion

The results obtained from the apparent rate constants for the charge transfer reaction of the  $Zn^{2+}/Zn(Hg)$  couple are in the same range as those obtained by previous investigators (11):

	<u>This work</u>	<u>Previous range</u>
1 <u>F</u> $NaClO_4$	$4.08 \times 10^{-3}$ cm/sec	$(3.6 - 4.01) \times 10^{-3}$ cm/sec
1 <u>F</u> $NaNO_3$	$4.02 \times 10^{-3}$ cm/sec	$(2.8 - 5.4) \times 10^{-3}$ cm/sec
1 <u>F</u> $NaCl$	$5.22 \times 10^{-3}$ cm/sec	$(4.0 - 16.0) \times 10^{-3}$ cm/sec

The present investigations have resulted in an increase in precision compared with previous determinations. For example, Lingane, using a potentiostatic technique (53), achieved a relative precision of only about 10% compared to the 3% level which was obtained in these investigations.

The increase in precision is largely due to the increase in precision with which the kinetic data could be obtained through the utilization of the computerized data acquisition system. The fact that a greater number of data points could be obtained from a single kinetic experiment, and the fact that several duplicate experiments could be done more rapidly also contributed to the increase in precision of these results compared to the earlier results.

The rate constants, both apparent and standard, obtained in nitrate and perchlorate media were the same within experimental error and significantly smaller than the corresponding constants

obtained in chloride media (Table XVI). This difference has been previously noted (54, 16, 55, 14) and several possible explanations have been advanced to rationalize this difference (12, 55, 56). The limited amount of data obtained in this study is unfortunately insufficient to warrant additional speculations on this topic here. However, it does seem justified to compare the quality of the data which has been obtained in this study, with that which has been obtained by other investigators in order to determine how well the conclusions that were reached by the investigators are borne out by the data. The method which has been given in this thesis for determining the quality of the parameters obtained from experimental data is easily adaptable to other experimental conditions and techniques. Recently, Sluyters et al. (14) have undertaken kinetic measurements very similar to those discussed in this thesis using an a. c. technique. By obtaining the real and imaginary components of the electrode admittance at a fixed frequency as functions of the potential and concentration of  $Zn^{2+}$ , rate constants for the  $Zn^{2+}/Zn(Hg)$  couple were obtained in various supporting electrolytes. In perchlorate media they found that the standard rate constant as defined by Eq. (11) was independent of potential, while in chloride, bromide, and iodide media the same rate constants appeared to display a potential dependence. By using the same experimental conditions as these investigators one can calculate the expected precision of the rate constants which they obtained. If the double layer data for each supporting electrolytes is used to convert the apparent rate constants which Sluyters et al.

Table XVI

Supporting electrolyte	Apparent rate constants ( $k_s^a$ ) (cm/sec)
NaNO <sub>3</sub>	$4.02 \times 10^{-3}$
NaClO <sub>4</sub>	$4.08 \times 10^{-3}$
NaNO <sub>3</sub> , NaClO <sub>4</sub>	$4.05 \pm .08 \times 10^{-3}$ (2.0%)
NaCl (z = 2)	$5.22 \pm .13 \times 10^{-3}$ (2.5%)
	Standard rate constants ( $k_s$ ) (cm/sec)
NaNO <sub>3</sub>	$2.58 \times 10^{-4}$
NaClO <sub>4</sub>	$2.66 \times 10^{-4}$
NaNO <sub>3</sub> , NaClO <sub>4</sub>	$2.62 \pm .06 \times 10^{-4}$ (2.3%)
NaCl (z = 1.69)	$6.50 \pm .06 \times 10^{-4}$ (.9%)

(14) obtained into standard rate constants, one can compare their apparently potential dependent rate constants with a potential independent rate constant. By using the expected quality of the rate constant as a criterion one can determine if the differences are significant or whether it is possible to ascribe the apparent potential dependence to the lack of quality of the data. These calculations were undertaken (Appendix A) and the results are shown in Table XVII. For these calculations a precision of 1% was assumed for measurement of the electrode admittance and except for iodide media, for which double layer data were obtained (57), the double layer was assumed to be the same as 1 F NaF. As can be seen in Table XVII the corrected rate constant in perchlorate appears independent of potential, while the rate constants for the other electrolytes appear to dependent on potential. However, only in bromide and iodide do the corrected rates deviate from the expected potential independent rate. The deviations are not significant at all the potentials and at the two potentials in bromide where the deviation is greater than one standard deviation it is still less than two standard deviations away from the potential independent rate. In iodide the expected precision decreases rapidly with increasing distance from the standard potential. However near the standard potential the deviation between the potential independent rate and the measured rate is significant. In summary, although the rate constant appears to be a function of potential in chloride, bromide, and iodide, an analysis of the experimental conditions that were used, indicates that except for iodide and possibly bromide the

Table XVII

Rate constant (cm/sec $\times 10^3$ )					
(E-E <sup>0</sup> )	Expected	Actual	Δ	Expected	Δ
I <sup>-</sup>	0	125	125	0	$\pm 8$
	-50	125	76	-49	$\pm 16$
	-100	125	35	-90	$\pm 181$
	-150	125	22	-103	$\pm 972$
	-200	125	14	-111	$\pm 4240$
Br <sup>-</sup>	0	11	11	0	$\pm .9$
	-50	11	14	+3	$\pm 4.4$
	-100	11	7.9	-3.1	$\pm 5.9$
	-150	11	4.4	-6.6	$\pm 5.0$
	-200	11	3.5	7.5	$\pm 6.5$
	-300	11	3.7	7.3	$\pm 53.7$
Cl <sup>-</sup>	0	6.3	6.3	0	$\pm 1.58$
	-50	6.3	6.67	.37	$\pm 6.62$
	-100	6.3	6.55	.25	$\pm 5.54$
	-150	6.3	4.23	-2.07	$\pm 3.40$
	-200	6.3	3.45	-2.85	$\pm 2.84$
	-300	6.3	3.22	-3.08	$\pm 10.71$
ClO <sub>4</sub> <sup>-</sup>	0	3.6	3.6	0	$\pm 16.20$
	-50	3.6	3.74	.14	$\pm 24.48$
	-100	3.6	3.68	.08	$\pm 10.44$
	-150	3.6	3.64	.04	$\pm 4.32$
	-200	3.6	3.68	.08	$\pm 2.12$
	-300	3.6	3.59	-.01	$\pm 1.19$

expected quality of the data is not good enough to exclude the possibility that the apparent potential dependence of the rate constants is in fact due only to the usual Frumkin double layer effect (24).

The main thrust of the work undertaken in this thesis was the detailed examination of the effects of various experimental conditions upon the quality and amount of kinetic information that could be obtained from a electrode kinetic experiment with the goal of enhancing and maximizing this kinetic information. Since a definite conclusion about the difference of rates in various supporting electrolytes can be reached only when the various models have been thoroughly tested for a variety of experimental conditions, a knowledge of the quality of the kinetic data obtained under these various conditions will enable one to determine the necessary precision with which the data must be obtained. One step toward increasing the precision of the kinetic data has been the utilization of the digital data acquisition system that is described in this thesis. This system has made possible not only the increased precision of the kinetic data but also it has proven a convenient and powerful tool with which to undertake fairly sophisticated and complex types of analysis in a comparatively short time. At the present time the overall response of digital acquisition system is limited by the time response of the general purpose electrochemical instrument that is used. A new instrument whose response time is significantly faster has been designed and constructed. With the addition of this instrument to the digital data acquisition system it is likely that the increased time response will

enable kinetic systems to be studied over more extended ranges of potentials making possible more definite conclusions about effects on charge transfer rates such as those produced by varying the electrolytes.

## References

1. P. Delahay, "New Instrumental Methods in Electrochemistry", Interscience, New York, 1954, pp. 28-45.
2. P. Delahay, "Double Layer and Electrode Kinetics", Interscience, New York, 1965, pp. 153-67.
3. J. O'M. Bockris, "Modern Aspects of Electrochemistry", edited by Bockris and Conway, Butterworth, London, 1954, No. 1, pp. 180-276.
4. P. Delahay, "Advances in Electrochemistry and Electrochemical Engineering", edited by Delahay and Tobias, Interscience, New York, 1961, Vol. 1, pp. 238-318.
5. R. Parsons, Trans. Faraday Soc., 47, 1332 (1951).
6. W. H. Reinmuth, "Advances in Analytical Chemistry and Instrumentation", edited by Reilley, New York, 1960, Vol. 1, pp. 241-292.
7. B. Conway, "Theory and Principles of Electrode Processes", Ronald Press, New York, 1965.
8. R. A. Marcus, Ann. Rev. Phys. Chem., 15, 155 (1964).
9. J. O'M. Bockris and A. K. N. Reddy, "Modern Electrochemistry", Plenum Press, New York, 1970, Vol. 2, pp. 845-1140.
10. K. B. Oldham and R. A. Osteryoung, J. Electroanal. Chem., 11, 397 (1966).
11. N. Tanaka and R. Tamamushi, Electrochim. Acta, 9, 963 (1964). This article is a compilation of rate parameters of electrode reactions for various systems, including the  $Zn^{+2}/Zn(Hg)$  electrode reaction.
12. P. Delahay and A. Aramata, J. Phys. Chem., 66, 2208 (1962).
13. G. Gavioli and P. Papaff, Ric. Sci. Serie II Sez A, 1, 193 (1961).
14. P. Teppema, M. Sluyters-Rehbach, and J. H. Sluyters, J. Electroanal. Chem., 16, 165 (1968).

15. M. Sluyters-Rehbach, J. Breukel, and J. H. Sluyters, J. Electroanal. Chem., 19, 85 (1968).
16. N. S. Hush and J. Blockledge, J. Electroanal. Chem., 5, 420 (1963).
17. J. Koryta, Electrochim. Acta, 6, 67 (1962).
18. V. V. Losev and A. I. Molodov, Zh. Fiz. Khim., 35, 11 (1961).
19. J. O'M. Bockris and A. K. N. Reddy, op. cit., p. 872.
20. Ibid., 871, 917-926.
21. G. Gouy, Compt. Rend., 149, 654 (1910).
22. D. L. Chapman, Phil. Mag. (6), 25, 475 (1913).
23. O. Stern, Z. Elektrochem., 30, 508 (1924).
24. A. N. Frumkin, Z. Physik. Chem., 164A, 121 (1933).
25. H. Gerischer and W. Vielstich, Z. Physik. Chem. (Frankfort), 3, 16 (1955); W. Vielstich and H. Gerischer, Z. Physik. Chem., 4, 10 (1955).
26. J. H. Christie, G. Lauer, and R. A. Osteryoung, J. Electroanal. Chem., 7, 60 (1964).
27. "Handbook of Mathematical Functions", edited by M. Abramowitz and I. Stegun, Dover Publications, New York, 1965, p. 297.
28. N. R. Draper and H. Smith, "Applied Regression Analysis", Wiley, New York, 1966, pp. 263-273 (contains an extended bibliography).
29. P. Bevington, "Data Reduction and Error Analysis for the Physical Sciences", McGraw-Hill, New York, 1969.
30. N. R. Draper and H. Smith, op. cit., p. 273, 299.
31. W. Reinmuth, Anal. Chem., 38, 274R (1966).
32. F. Anson, Ann. Rev. Phys. Chem., 19, 83 (1968).
33. J. Osteryoung and R. A. Osteryoung, Electrochim. Acta, in press.

34. P. Lingane, Ph. D. Thesis, California Institute of Technology, 1966.
35. W. Deming, "Statistical Adjustment of Data", Wiley, New York, 1943.
36. R. A. Fisher, "Statistical Methods and Scientific Inference", Oliver and Boyd, Edinburgh, 1956.
37. R. A. Fisher, "Statistical Methods for Research Workers", Oliver and Boyd, Edinburgh, 1950.
38. G. Lauer, Ph. D. Thesis, California Institute of Technology, 1966, pp. 86-247.
39. G. Lauer, R. Abel, and F. Anson, Anal. Chem., 39, 765 (1967).
40. G. Lauer and R. A. Osteryoung, Anal. Chem., 39, 1866 (1967).
41. D. J. Fisher, Chemical Instrumentation, 2 (1), pp. 7-10 (1969).
42. N. Draper and H. Smith, op. cit., pp. 95-99.
43. P. Bevington, op. cit., pp. 313-316.
44. L. Sillen and B. Liliequist, Svensk Kim. Tidskr., 56, 85 (1944).
45. G. Lauer and R. Osteryoung, Anal. Chem., 38, 1106 (1966).
46. D. Grahame and R. Parsons, J. Amer. Chem. Soc., 83, 1291 (1961).
47. D. Grahame, J. Amer. Chem. Soc., 76, 482 (1954).
48. L. Sillen and A. Martell, "Stability Constants of Metal Ion Complexes", The Chemical Society, London, 1964.
49. C. Russell, J. Electroanal. Chem., 6, 486 (1963).
50. R. Payne, J. Phys. Chem., 69, 4113 (1965).
51. R. Payne, J. Phys. Chem., 70, 204 (1966).
52. P. Bevington, op. cit., p. 56.

53. P. Lingane and J. Christie, J. Electroanal. Chem., 10, 284 (1965).
54. R. Tamamushi, R. Ishibashi, and N. Tanaka, Z. Physik. Chem. N. F., 35, 209 (1962); 39, 117 (1963).
55. J. Randles and K. Somerton, Trans. Faraday Soc., 48, 951 (1952).
56. R. Parsons, J. Electroanal. Chem., 21, 35 (1969).
57. D. Grahame, J. Amer. Chem. Soc., 80, 4201 (1958).
58. M. Sluyters-Rehbach and J. Sluyters, "Electroanalytical Chemistry", ed. A. Bard, Marcel Dekker, Inc., New York, 1970, Vol. 4, pp. 1-121.
59. N. Draper and H. Smith, op. cit., p. 18.

APPENDIX A  
Error Analysis for Kinetic Data Obtained  
by Faradaic Impedance

The two components of the electrode admittance are defined as (58)

$$Y_{e1}^1 = \frac{\omega^{1/2}}{s} \frac{p + 1}{p^2 + 2p + 2} \quad (1)$$

$$Y_{e1}^1 = \frac{\omega^{1/2}}{s} \frac{1}{p^2 + 2p + 2} + \omega Cd \quad (2)$$

where

$$p = \frac{(2\omega)^{1/2}}{k_a} \frac{1}{[D_O^{-1/2} \exp(-\alpha\varphi) + D_r^{-1/2} \exp[(1-\alpha)\varphi]]} \quad (3a)$$

$$s = \frac{RT}{n^2 F^2 C_O \sqrt{2}} \frac{\left[ 1 + a_O \exp(\alpha\varphi) + \left( \frac{D_O}{D_r} \right)^{1/2} \exp(\varphi) \right]}{\left[ \alpha a_O + \left( \frac{D_O}{D_r} \right)^{1/2} \exp[(1-\alpha)\varphi] \right]} * \quad (3b)$$

$$\left[ D_O^{-1/2} \exp(-\alpha\varphi) + D_r^{-1/2} \exp[(1-\alpha)\varphi] \right]$$

$$\varphi = \frac{nF}{RT} (E - E^0)$$

$$a_O = \left( \frac{D_O}{\pi t} \right)^{1/2} \frac{1}{k_a}$$

$\omega$  = frequency of the alternating potential

$C_d$  = double layer capacity

Equation (1) and Eq. (2) can be combined to yield

$$Y_{e1}^{11} = \frac{Y_{e1}^1}{p+1} + \omega C_d \quad (4)$$

It can be seen by examining Eq. (3a) and Eq. (3b) that  $p$  is independent of the concentration of the oxidized species,  $C_o$ , while  $s$  is inversely proportional to the concentration of the oxidized species.

Thus if the two components of the electrode admittance are determined for a series of concentrations of 0 at constant frequency and at constant potential, a plot of  $Y_{e1}^{11}$  against  $Y_{e1}^1$  will have a slope given by  $\frac{1}{1+p}$ , from which  $p$  can be determined. If the determination of  $p$ , by concentration variation, is carried out over a series of potentials, the resulting values of  $p$  can be used to calculate a rate constant through the use of Eq. (3a).

If the assumption is made that the values  $Y_{e1}^1$  are more precise than the values of  $Y_{e1}^{11}$ , the error analysis becomes very simple and is that of a line having a slope and intercept to be determined by a linear least-squares analysis. The assumption that  $Y_{e1}^1$  is much more precise than  $Y_{e1}^{11}$  may not be completely valid. However this assumption will allow the imprecision of the determined parameters to be calculated easily.

For the least-squares analysis of a straight line with a slope and intercept, the expected standard error of the slope in terms of

the standard error of the dependent variable and the values of the independent variables used in the analysis is given by (59)

$$\sigma_{\text{slope}} = \frac{1}{\sqrt{\sum x^2 - \frac{(\sum x)^2}{n}}} \sigma_Y \quad (5)$$

For the particular case being discussed, the slope corresponds to

$\frac{1}{1+p}$ , the independent variable to  $Y_{e1}^1$ , and the dependent variable,  $Y$ , to  $Y_{e1}^{11}$ .

The form of Eq. (5) is not the final desired form since we are interested in the imprecision of the rate constant,  $k_a$ , which is calculated from the slope. By using the law of propagation of errors (52) the final form can be obtained. From Eq. (3a), we obtain:

$$\frac{\sigma_{k_a}}{k_a} = \frac{\sigma_p}{p} \quad (6a)$$

and if we define the slope as  $m$ , we obtain

$$\frac{\sigma_p}{p} = \frac{1}{m(1-m)} \sigma_m \quad (6b)$$

Combining Eq. (6a) and Eq. (6b) with Eq. (5) we obtain:

$$\frac{\sigma_{k_a}}{k_a} = \frac{1}{m(1-m)} \frac{1}{\sqrt{\sum x^2 - \frac{(\sum x)^2}{n}}} \sigma_Y \quad (7)$$

$$\text{where } m = \frac{1}{1+p}$$

$$x = Y_{e_1}^{11}$$

$$Y = Y_{e_1}^{11}$$

n = number of points analyzed.

Using Eq. (7), the expected precision of the rate constant can now be calculated by inserting the appropriate values corresponding to the particular experimental conditions.

The calculations which were performed in the main body of this thesis used the following values which were chosen to correspond to the experimental conditions used by Sluyters et al. (14):

$$\text{frequency} = 1 \times 10^3 \text{ Hz}$$

$$D_O = \frac{D_r}{2} = 8 \times 10^{-6}$$

$$C_d = 20 \times 10^{-6} \text{ F/cm}^2$$

$$t = 3 \text{ sec}$$

$$\alpha = 0.19$$

$$C_O = 1 \times 10^{-3}, 5 \times 10^{-3} \text{ M for } I^-$$

$$1 \times 10^{-2}, 2 \times 10^{-2} \text{ M for } Cl^-, Br^-, ClO_4^-$$

A precision of 1% was assumed for  $Y_{e_1}^{11}$  and the values of expected precision of the apparent rate constants were calculated for values of  $(E - E^0)$  equal to 0, -50, -100, -150, -200, -300 mV.

## APPENDIX B

## Computer Programming for Data Acquisition and Analysis

Because programming considerations are relatively important for utilization of a computer for control, data acquisition, and analysis and because a considerable amount of time has been spent in writing programs of this type, I will use the remainder of this section to discuss the general features of a data acquisition, analysis, and control program and illustrate these features with an example that has been used for experiments investigating electrode kinetics.

There are four sections in a program of this type

- (1) Initial input
- (2) Data acquisition
- (3) Data analysis
- (4) Final output

The contents of each of the sections varies with the particular technique to be utilized and there may be some overlapping of the sections. However all programs of this type will have these sections.

The first section handles the input of those parameters which are necessary to define the experiment and scale the data or convert it into a meaningful form. The parameters defining the experiment are such things as the number of points to be taken, the sampling rate, and which of the data points are included in the analysis.

When memory capacity is adequate the input is arranged to be in a form most meaningful and easily interpreted by the experimenter.

The second section, data acquisition, is executed in real time, so that synchronization with the experiment is essential. The amount of testing of the data as it is received that is possible, depends on the efficiency of the programmer and the sampling rate employed. If the testing operation takes too long data may be lost or synchronization destroyed. In the experiments described here very little real time computation was necessary. About the only thing that had to be done was to keep track of the number of iterations and test the data to see if it was exceeding the full scale range of the A. D. C. However, some additional refinements were added to make more efficient use of time, since the computer would otherwise have spent a great deal of its time waiting for data. For example, when ensemble averaging was used the data were often averaged as they were acquired.

The sequence of actions in this section of the program take place in the following way. First, the experiment is initiated, then data are acquired and testing takes place. This includes the test as to whether another point is to be taken or whether the experiment is to be terminated. If more data are to be acquired the computer returns to that step and waits for the data. If the desired amount of data has been acquired the experiment is terminated and conditions are reset to the initial conditions.

The third program section is concerned with the analysis of the data that have been obtained. After scaling, the sampling rate is utilized to obtain the functionalized independent variables (if a function of time is the independent variable). The data points chosen

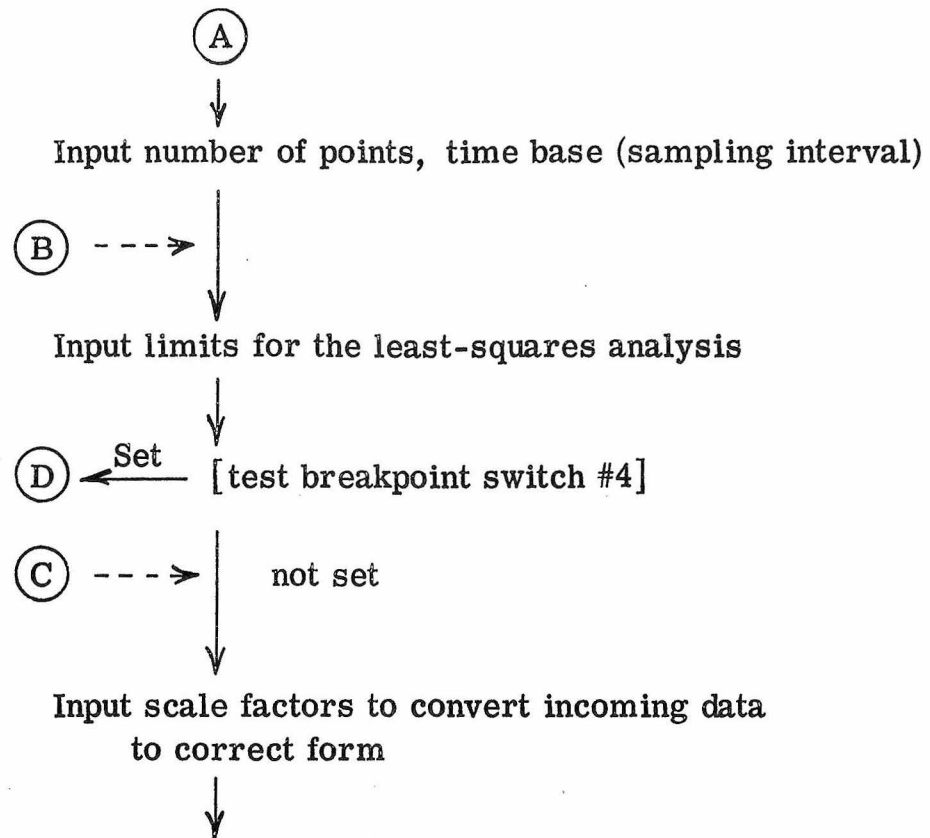
for analysis (in section one) are then analyzed with an appropriate regression method and the desired parameters and their associated variances are determined.

In the final section the parameters evaluated are typed out along with any additional desired information such as goodness of fit. The flow of information between the computer and operator may take place on any of the devices available for this. In our system this is via the typewriter although displays generated by the computer and shown on an oscilloscope or x-y recorder have also been utilized. The typewriter is used most often because it provides for two way communication that is easily intelligible to the operator and also provides a hard copy for the operator.

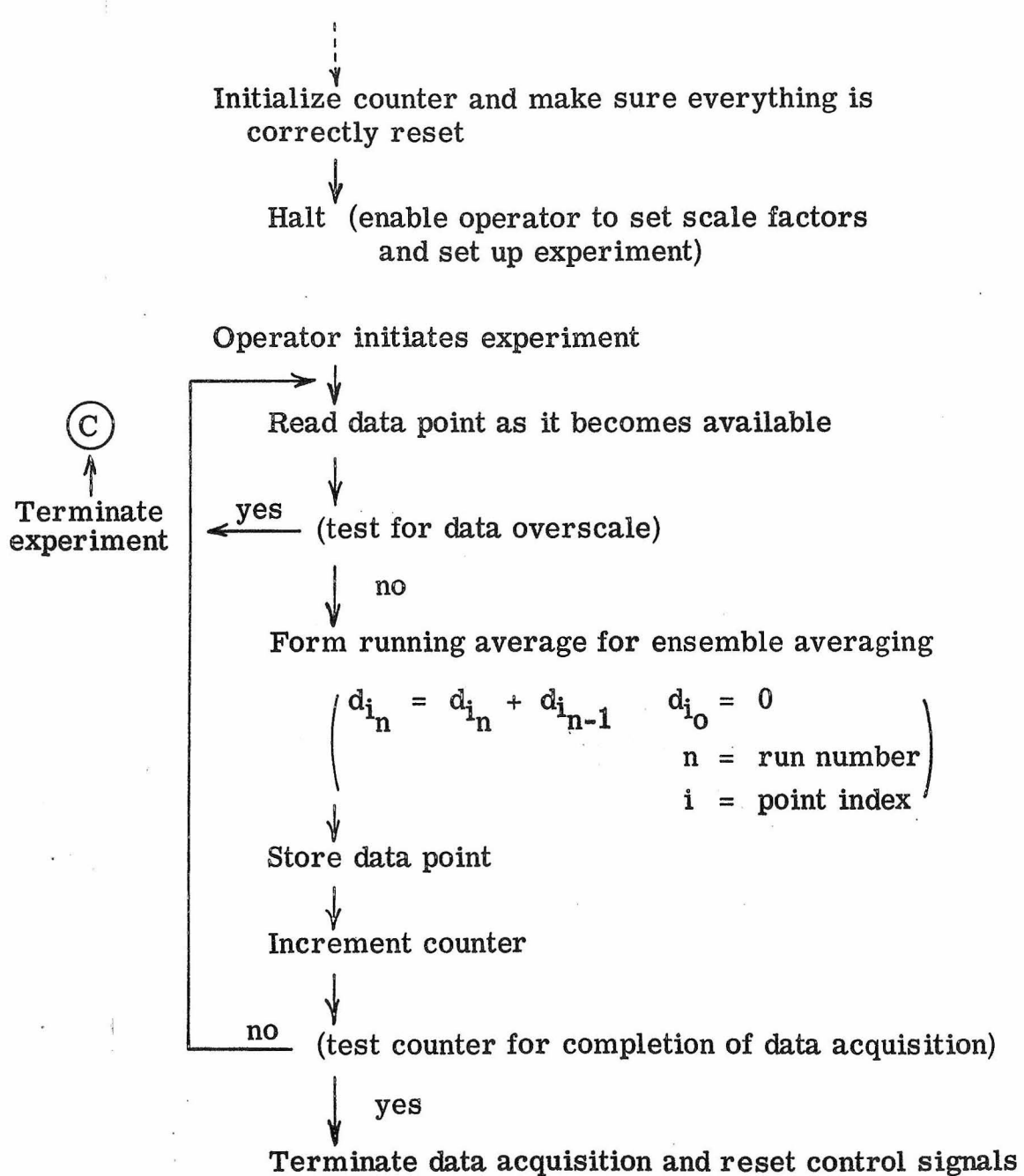
These sections that have been discussed will be illustrated in detail by the program which has been written for studies of electrode kinetics.

The kinetic program will be written in the form of a flow diagram. The flow diagram is useful because the general features of the program can be illustrated in a way that is independent of the particular computer used. This should serve to make the program meaningful to someone who is not familiar with the particular command structure of the computer that was used in this research. A program listing is available upon request. However, since it has been written in an assembly language it can only be used on the particular system used in these studies.

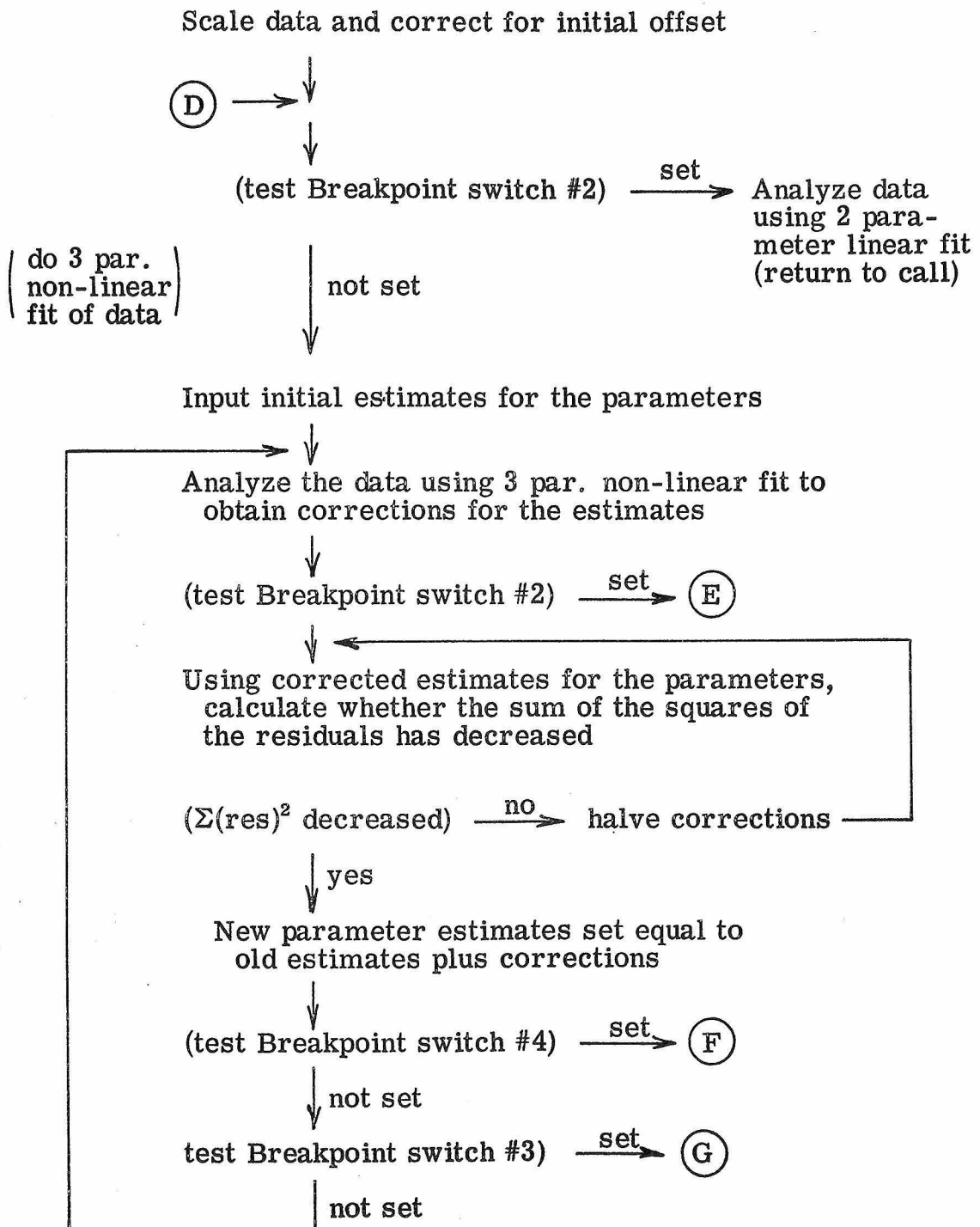
## Initial Input (Section 1)

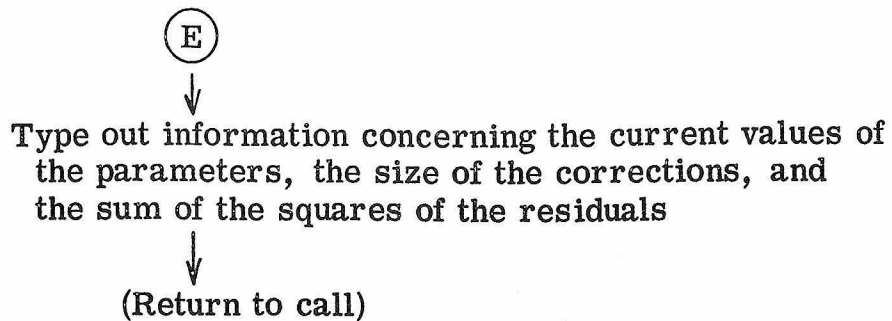


## Data Acquisition (Section 2)



## Analysis (Section 3)





### Final Typeout (Section 4)

